

DUST ABSORPTION AND THE ULTRAVIOLET LUMINOSITY DENSITY AT $Z \approx 3$ AS CALIBRATED BY LOCAL STARBURST GALAXIES¹

GERHARDT R. MEURER, TIMOTHY M. HECKMAN

The Johns Hopkins University, Department of Physics and Astronomy,
Baltimore, MD 21218-2686

Electronic mail: meurer@pha.jhu.edu, heckman@pha.jhu.edu

AND

DANIELA CALZETTI

Space Telescope Science Institute, 3700 San Martin Drive, Baltimore, MD 21218

Electronic mail: calzetti@stsci.edu

Astrophysical Journal, accepted 27 Feb., 1999

ABSTRACT

We refine a technique to measure the absorption corrected ultraviolet (UV) luminosity of starburst galaxies using rest frame UV quantities alone, and apply it to Lyman-limit U -dropouts at $z \approx 3$ found in the Hubble Deep field (HDF). The method is based on an observed correlation between the ratio of far infrared (FIR) to UV fluxes with spectral slope β (a UV color). A simple fit to this relation allows the UV flux absorbed by dust and reprocessed to the FIR to be calculated, and hence the dust-free UV luminosity to be determined. *International Ultraviolet Explorer* spectra and *InfraRed Astronomical Satellite* fluxes of local starbursts are used to calibrate the F_{FIR}/F_{1600} versus β relation in terms of A_{1600} (the dust absorption at 1600Å), and the transformation from broad band photometric color to β . Both calibrations are almost completely independent of theoretical stellar population models. We show that the recent marginal and non-detections of HDF U -dropouts at radio and sub-mm wavelengths are consistent with their assumed starburst nature, and our calculated A_{1600} . This is also true of recent observations of the ratio of optical emission line flux to UV flux density in the brightest U -dropouts. This latter ratio turns out *not* to be a good indicator of dust extinction. In U -dropouts, absolute magnitude $M_{1600,0}$ correlates with β : brighter galaxies are redder, as is observed to be the case for local starburst galaxies. This suggests that a mass-metallicity relationship is already in place at $z \approx 3$. The absorption-corrected UV luminosity function of U -dropouts extends up to $M_{1600,0} \approx -24$ ABmag corresponding to a star formation rate $\sim 200 M_{\odot} \text{ yr}^{-1}$ ($H_0 = 50 \text{ km s}^{-1} \text{ Mpc}^{-1}$, $q_0 = 0.5$ assumed throughout). The absorption-corrected UV luminosity density at $z \approx 3$ is $\rho_{1600,0} \geq 1.4 \times 10^{27} \text{ erg s}^{-1} \text{ Hz}^{-1} \text{ Mpc}^{-3}$. It is still a lower limit since completeness corrections have not been done and because only galaxies with $A_{1600} \lesssim 3.6$ mag are blue enough in the UV to be selected as U -dropouts. The luminosity weighted mean dust absorption factor of our sample is 5.4 ± 0.9 at 1600Å.

Subject headings: galaxies: starburst – early universe – ultraviolet: galaxies – infrared: galaxies – radio continuum: galaxies

1. INTRODUCTION

In the past few years we have seen the fruition of a great astronomical endeavour: the measurement of the rate of cosmological evolution via direct censuses of star formation tracers, metal content, and metal production rate (Lilly et al. 1995; Pei & Fall 1995; Lilly et al. 1996; Madau et al. 1996; Connolly et al. 1997; Madau, Pozzetti, & Dickinson 1998). This achievement has come about thanks to several key developments including (1) deep sub-arcsecond imag-

ing capabilities, especially in the optical with the *Hubble Space Telescope* (Williams et al. 1996), (2) multi-object spectroscopy, especially down to $V \approx 26$ ABmag with the 10m Keck telescopes (e.g. Steidel et al. 1996a,b; Lowenthal et al. 1997), and (3) the refinement of photometric redshift techniques (e.g. Connolly et al., 1997) especially the Lyman-limit technique (e.g. Steidel & Hamilton 1992; Steidel, Pettini, & Hamilton 1995) which allow redshift estimates

¹Based on observations with the NASA/ESA *Hubble Space Telescope* obtained at the Space Telescope Science Institute, which is operated by the Association of Universities for Research in Astronomy, Inc., under NASA contract NAS5-26555.

to be made to greater depth, and out to $z \approx 5$.

In a pioneering paper Madau et al. (1996; hereafter M96) derived the z evolution of the metal production rate $\dot{\rho}_Z(z)$ (in comoving coordinates), which is directly proportional to the volume density of the star formation rate (SFR). The ‘‘Madau plot’’ provides a direct constraint on the evolution of galaxies, hence it’s importance. It shows a strong (factor ~ 10) decline in $\dot{\rho}_Z(z)$ from its peak at $z \approx 1 - 2$ to the present epoch, as pointed out earlier by Lilly et al. (1996). This decline mirrors that seen in the luminosity density of quasars (Boyle & Terlevich 1997). On the other side of the peak, at $z \approx 4$, $\dot{\rho}_Z(z)$ is apparently only equal to that of the present epoch. Subsequent work by Connolly et al. (1997) fills in the $z = 1 - 2$ gap and is consistent with M96. The overall shape of the curve is consistent with models of the observed evolution in the properties of damped Lyman- α systems (Pei & Fall, 1995). This form for $\dot{\rho}_Z(z)$ is consistent with hierarchical models of galaxy formation (e.g. Searle & Zinn, 1978; Zepf & Ashman, 1993; Baugh et al. 1998).

One concern about the Madau plot is that it is heavily biased to observations in the rest frame UV. The problem is that dust efficiently scatters and absorbs UV radiation, greatly complicating the interpretation of the detected UV emission. Not only is the amount of dust important, but so is the geometry (where it is relative to the stars), and the composition of the dust. For example, in the Local Group the UV ‘‘extinction law’’ varies from galaxy to galaxy and within galaxies, (e.g. Fitzpatrick 1986). The term ‘‘extinction law’’ was originally defined for stars. It quantifies the wavelength dependent combined effect of dust absorption and scattering out of the line of sight toward point sources. The geometry is quite different in distant galaxies where individual stars can not be isolated, and instead galaxies in their entirety, or large portions of them are observed. In such cases much of the scattered light may be recovered (by scattering into the line of sight), and it matters a great deal how porous the dust distribution is and whether the stars are mixed with the dust or not (e.g. Witt, Thronson, & Capuano 1992; Calzetti, Kinney & Storchi-Bergmann 1994). There are a variety of terms for the wavelength dependent net dimming of the light including ‘‘effective extinction law’’ (Calzetti et al. 1994) and ‘‘obscuration law’’ (Calzetti 1997). Here we adopt the term ‘‘absorption law’’ to emphasize that it is dust absorbing photons that causes the dimming. Absorption laws can be derived empirically (e.g. Calzetti et al. 1994; Calzetti 1997) and hence average together all the above geometric factors into a simple wavelength dependent correction.

Observations of high redshift galaxies in the sub-mm and mm bands prove that molecular gas and dust formation have occurred as far back as $z = 4.7$ (Omont et al. 1996; Ivison et al. 1998; Guilloteau et al. 1997; Frayer et al. 1999). Especially interesting are the recent spate of blank field sub-mm detection with SCUBA, which we discuss in more detail in §5.2 and §6.3. These can account for a significant fraction of the sub-mm background, and are mostly attributed to dusty star forming galaxies having $z > 1$. Following from UV observations of local starbursts (Meurer et al. 1995, hereafter Paper I) we have argued that the correction factor to $\dot{\rho}_Z(z)$ is considerable, a factor ~ 15 at $z \approx 3$ (Meurer et al., 1997; hereafter Paper II), while others (e.g. Madau 1997; Pettini et al. 1997) prefer fairly modest, \sim factor of three, corrections. The amount of high- z absorption has a direct bearing on the interpretation of the Madau plot; large corrections at high- z can push back the peak $\dot{\rho}_Z$, as might be expected by monolithic collapse dominated galaxy formation (e.g. Eggen, Lynden-Bell, & Sandage 1962; Bower, Lucey & Ellis 1992; Ortolani et al. 1995).

Here we reexamine the UV luminosity density at high- z , with particular emphasis on the U -dropouts in the HDF. Our technique has two strengths. Firstly, it is based on the similarity between local starburst galaxies and Lyman limit systems as summarized in § 2. The main assumption we make is that the high redshift galaxies have the same multi-wavelength spectral properties as local starbursts. We use local starburst galaxies to calibrate the relationship between UV reddening and UV absorption (in § 3) thus largely avoiding the uncertainties in population model fitting and the choice of effective UV absorption laws. Secondly, our calibration of the UV absorption law recovers the intrinsic (i.e. dust-free) UV emission that is absorbed by dust and reradiated in the far infrared. Hence, up to the modest amounts of absorption considered here (a few magnitudes), UV observations are capable of recovering the total bolometric luminosity of starbursts. We apply our calibrations to the U -dropouts in the HDF in § 4. In § 5 we demonstrate the validity of our starburst assumption by showing that new constraints on the SEDs of these high- z systems are consistent with the SEDs of local UV selected starbursts. Implications of our results are discussed in §6, while § 7 summarizes the paper.

Throughout this paper we adopt $H_0 = 50 \text{ km s}^{-1} \text{ Mpc}^{-1}$, $q_0 = 0.5$.

2. HIGH-Z GALAXIES AND LOCAL STARBURSTS

Progress in understanding the Lyman-dropout galaxies would be accelerated if we could find analogs to these galaxies in the local universe. Fortunately,

there is mounting evidence that the Lyman dropout galaxies indeed resemble starburst galaxies in many respects.

While the magnitude of the extinction corrections to the rest-frame UV light (the subject of the present paper) is still a matter of debate, it is nevertheless clear that local starbursts have surface-brightnesses that are similar to the distant galaxies (Paper II). That is, the high- z galaxies appear to be ‘scaled-up’ versions of the local starbursts with the same SFRs per unit area and comparable stellar surface-mass-densities. In this regard, starbursts are a far better match to the Lyman-dropout galaxies than are ordinary late-type galaxies, which have SFRs per unit area that are several orders-of-magnitude smaller (cf. Paper II; Kennicutt 1998).

The overall rest-frame UV-through-optical spectral properties of local starbursts and the Lyman dropout galaxies are similar in terms of the spectral energy distribution (cf. Sawicki & Yee 1998) and the dominance of the UV and optical spectra by absorption and emission lines respectively (cf. Leitherer 1997; Pettini et al. 1998). The Lyman limit systems in the HDF are clearly spatially resolved (Giavalisco, Steidel, & Macchetto 1996), demonstrating that their rest frame UV light is not dominated by an AGN. In addition the spectra of the Lyman-dropout galaxies is more similar to starburst galaxies than AGN. Indeed the typical strengths of the UV stellar and interstellar absorption-line features are comparable in starbursts and Lyman-dropout galaxies, indicative of broadly similar stellar and interstellar content (e.g. Conti, Leitherer, & Vacca 1996; Lowenthal et al. 1997). The local starbursts and Lyman dropout galaxies also have similar distributions of observed UV colors, (Paper II, and here in §4), - which we argue chiefly measures the amount of dust-reddening.

Even the dynamical state of the interstellar medium in the Lyman dropout galaxies resembles that in local starbursts. Both are driving extensive outflows of gas at velocities of several hundred km s^{-1} . The signature of this is the systematic blueshift of the broad UV interstellar absorption-lines with respect to the rest-frame optical (e.g. $\text{H}\beta$) and/or rest-frame UV ($\text{Ly}\alpha$) nebular emission-lines (Pettini et al. 1998; Franx et al. 1997; Kunth et al. 1998; Gonzalez-Delgado et al. 1998). The velocity dispersion of the emission-line gas is also similar in the two galaxy classes (Pettini et al. 1998).

To reiterate, in all their properties measured to date, the Lyman dropout galaxies appear to be simply scaled-up versions of local starbursts: larger and more luminous, but otherwise remarkably similar. The challenge is to determine the intrinsic luminosities from the UV fluxes and colors of dusty Lyman

limit systems. The above similarities justifies our approach of calibrating the effects of dust on local starbursts and applying it to the high- z galaxies.

3. THE LOCAL SAMPLE CALIBRATION

Figure 1 illustrates the heart of the technique. It shows the relationship between the ratio of far infrared (FIR) and ultraviolet (UV) fluxes (here at 1600\AA) and the UV spectral slope β (equivalent to a color) for a sample of starburst galaxies. Since the FIR flux is due to dust radiatively heated by the absorbed UV radiation, the y axis is a measurement of dust absorption. This figure then shows that dust absorption is correlated with UV reddening. Such a relationship is expected for dust predominantly located in a foreground screen (Witt et al. 1992; Paper I), although this screen need not be homogeneous (Calzetti et al. 1994; Calzetti 1997). Because this correlation links F_{FIR} to UV quantities, then regardless of the exact dust geometry, this figure provides a powerful *empirical* tool for recovering the radiation reprocessed by dust and thus determining the total absorption-corrected UV flux of starbursts, using UV quantities alone.

In the next sub-section we define our local calibrating samples and the quantities we use. In order to apply this tool and interpret the results we perform three calibrations. 1. F_{FIR}/F_{1600} is calibrated in terms of absorption at 1600\AA and this is fitted as a function of β . 2. The spectroscopic index β is calibrated in terms of broad-band colors (with a z correction), since photometric colors are easier to measure than spectroscopic ones. 3. The relationship between luminosity measured at 1600\AA is related to SFR. These calibrations are detailed in the final three sub-sections.

3.1. Sample and definitions

The local sample used to derive the various calibrations in this paper is listed in Table 1. It includes the sources shown in Fig. 1, and is drawn from the *International Ultraviolet Explorer* (IUE) atlas of Kinney et al. (1993), and contains galaxies having an ‘‘activity class’’ consistent with being a starburst, i.e. SB nuc. (starburst nucleus), SB ring (starburst ring), BCDG (blue compact dwarf galaxy), or BCG (blue compact galaxy). Although the UV sources in these galaxies tend to be centrally concentrated we find that galaxies with optical diameters $D_{25} > 4'$ (D_{25} is measured at $B = 25 \text{ mag arcsec}^{-2}$) tend to fall above the relationship shown in Fig. 1. This is probably because significant UV emission extends beyond the $20'' \times 10''$ IUE aperture. Hence these large galax-

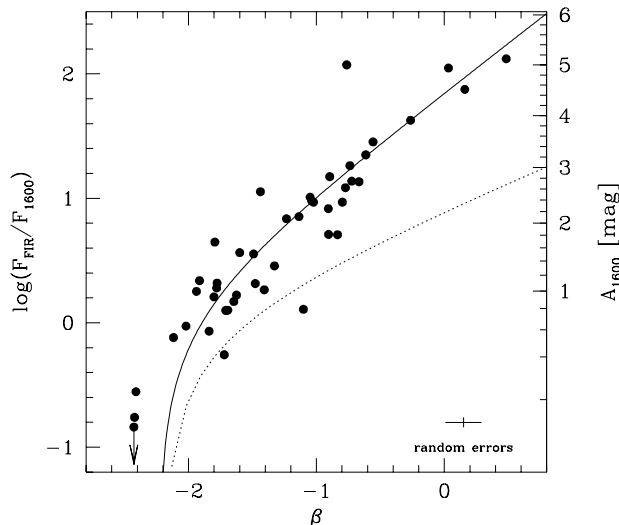


FIG. 1.— The ratio of FIR to UV flux at 1600\AA compared to UV spectral slope β for UV selected starburst galaxies. The right axis converts the flux ratio to 1600\AA absorption A_{1600} using eq. 11. The solid line shows our adopted linear fit to the A_{1600} , β relationship. The dotted line shows the proposed dust absorption/population model of Pettini et al. (1997).

ies were excluded from the sample². Further limiting the sample to galaxies having $D_{25} < 2.5'$ removes a few more outliers, but not just galaxies above the relationship. Furthermore, it also severely depletes the points with $\beta > -0.5$. Applying fits to data limited in this way changes our final $\rho_{1600}(z = 2.75)$ results by $< 10\%$, hence we retain $D_{25} < 4'$ as the diameter limit for the local sample. The lack of systematic residuals for galaxies up to 12 times larger than the IUE aperture indicates that the UV emission of these galaxies is very compact, e.g. in a circum-nuclear starburst.

The IUE spectra in the Kinney et al. atlas were measured to determine the UV quantities required for Fig. 1. The ultraviolet flux at 1600\AA , F_{1600} is a generalized flux of the form $F_{\lambda} = \lambda f_{\lambda}$, and f_{λ} is the flux density per wavelength interval. It was measured with the *IRAF* / *STSDAS*³ package *SYNPHOT* employing a square passband with a central wavelength of 1600\AA and width of 350\AA . This filter is meant to approximate the rest frame parameters of the standard WFPC2 filters F606W and F814W for objects

with redshifts $z = 2.75$, and 4, respectively (i.e. *U* and *B* band dropouts). The ultraviolet spectral slope β is determined from a power law fit of the form

$$f_{\lambda} \propto \lambda^{\beta}. \quad (1)$$

to the UV continuum spectrum as defined by the ten (rest wavelength) continuum bands listed by Calzetti et al. (1994). These spectral fits were performed after first removing Galactic extinction using the law of Seaton (1979) and taking Galactic extinction values $A_B = 4.1E(B - V)$ from Burstein & Heiles (1982, 1984) as listed by NED⁴. Since the continuum spectrum is never exactly a pure power law, β is subject to systematic uncertainties due to the placement of the continuum windows. Eighteen of the data points in Fig 1 represent galaxies observed with one of IUE's short wavelength (SW) cameras ($\lambda \approx 1100\text{\AA}$ to 1975\AA) only and not with either of the LW cameras ($\lambda \approx 1975\text{\AA}$ to 3000\AA), hence they do not have data in Calzetti's et al. (1994) tenth window ($\lambda = 2400 - 2580\text{\AA}$). Their β values were determined from the SW only measurements using the following

²The other galaxies that were excluded are NGC 1569 because of excessive foreground Galactic extinction; NGC 3690 because the IUE pointing is likely to be wrong (Paper I); the BCDGs Mrk209, Mrk220, and Mrk499 because they have neither IRAS fluxes nor upper limits; and finally five galaxies with low S/N IUE spectra in the Kinney et al. atlas: NGC 4853, IC 2184, Mrk 309, Mrk 789, UGC 6448.

³The *Image Reduction and Analysis Facility* software package is distributed by the National Optical Astronomy Observatories, which are operated by the Association of Universities for Research in Astronomy, Inc., under cooperative agreement with the National Science Foundation. *STSDAS* is the *Space Telescope Science Data Analysis Software* package for *IRAF*, distributed by STScI.

⁴The NASA/IPAC Extragalactic Database (NED) is operated by the Jet Propulsion Laboratory, California Institute of Technology, under contract with the National Aeronautics and Space Administration.

TABLE 1
LOCAL SAMPLE: RELEVANT DATA

name	$A_B(\text{Gal})$ [mag]	β	$\log(\frac{F_{\text{FIR}}}{F_{1600}})$	$\log(F_{\text{FIR}})$ [erg/cm ² /s]	$\log(\frac{F_{\text{H}\beta}}{f_{1600}})$ [Å]	$\frac{F_{\text{H}\alpha}}{F_{\text{H}\beta}}$	$\frac{F_{[\text{OIII}]5007}}{F_{\text{H}\beta}}$	Relevant figures
NGC 4861	0.00	-2.46	-0.08	-9.97	3
I Zw 18	0.02	-2.43	< -0.84	< -11.50	1,3
NGC 1705	0.18	-2.42	-0.76	-10.29	-0.01	2.85	4.61	1,7
Mrk 153	0.00	-2.41	-0.55	-10.92	1
Tol1924-416	0.30	-2.12	-0.12	-10.17	0.94	2.91	4.87	1,3,7
UGC 9560	0.00	-2.02	-0.03	-10.41	0.79	3.36	4.13	1,3,7
Mrk 66	0.01	-1.94	0.25	-10.56	0.68	2.85	2.90	1,7
NGC 3991	0.02	-1.91	0.34	-9.80	1,3
NGC 3738	0.00	-1.89	3
UGCA 410	0.02	-1.84	-0.07	-10.86	1
Mrk 357	0.17	-1.80	0.21	-10.37	0.80	3.25	...	1,7
NGC 3353	0.00	-1.79	0.65	-9.61	1,3
MRK 54	0.02	-1.78	0.28	-10.27	1
NGC 1140	0.11	-1.78	0.32	-9.77	0.96	3.18	2.66	1,7
Mrk 36	0.00	-1.72	-0.26	-10.94	1
MCG6-28-44	0.02	-1.77	0.31	-10.27	1
NGC 1510	0.00	-1.71	0.10	-10.36	0.67	3.11	4.95	1,3,7
MRK 19	0.14	-1.69	0.10	-10.64	1
NGC 4214	0.00	-1.69	3
NGC 4670	0.04	-1.65	0.17	-9.85	1,3
NGC 1800	0.00	-1.65	0.41	3.08	3.99	7
UGC 5720	0.00	-1.62	0.22	-9.97	1,3
UGC 5408	0.00	-1.60	0.56	-10.22	1
NGC 7673	0.14	-1.50	0.75	4.46	2.13	3,7
NGC 3125	0.25	-1.49	0.55	-9.64	1.07	3.28	4.72	1,7
Haro 15	0.08	-1.48	0.31	-10.16	0.74	2.85	2.32	1,7
NGC2537	0.15	-1.44	1.05	-9.73	1
UGC 3838	0.07	-1.41	0.26	-10.55	1
NGC 7793	0.00	-1.34	0.63	4.60	0.55	3,7
NGC 5253	0.18	-1.33	0.69	-8.86	1.02	3.18	4.68	3,7
NGC 7250	0.62	-1.33	0.46	-9.77	0.80	3.14	3.48	1,7
Mrk 542	0.07	-1.32	0.54	4.00	0.79	7
NGC 7714	0.15	-1.23	0.84	-9.32	1.18	4.36	1.60	1,3,7
Mrk 487	0.02	-1.15	1.01	3.25	6.61	7
NGC 3049	0.04	-1.14	0.85	-9.84	0.99	4.00	0.23	1,7
UGC 6456	0.09	-1.10	0.11	-10.74	1
NGC 3310	0.00	-1.05	1.01	-8.83	1
NGC 5996	0.06	-1.04	0.98	-9.64	0.86	4.76	0.38	1,7
NGC 4385	0.03	-1.02	0.97	-9.65	0.97	5.48	0.79	1,7
Mrk 499	0.00	-1.02	0.38	4.65	3.57	7
NGC 5860	0.03	-0.91	0.92	-10.04	0.88	6.04	0.64	1,7
IC 1586	0.07	-0.91	0.71	-10.28	0.89	5.30	1.35	7
NGC 2782	0.00	-0.90	1.17	-9.33	1
ESO383-44	0.13	-0.83	0.71	-10.13	1
NGC 5236	0.14	-0.83	0.69	3.91	0.22	7
NGC 2415	0.16	-0.80	0.97	-9.36	1
MCG-01-30-33	0.05	-0.77	1.09	-9.84	1
NGC 1614	0.22	-0.76	2.07	-8.84	1.24	7.85	0.96	7
NGC 6217	0.14	-0.74	1.26	-9.22	0.79	5.08	0.39	1,7
NGC 6052	0.10	-0.72	1.14	-9.48	1.04	3.54	2.01	1,7
NGC 4500	0.00	-0.67	1.13	-9.69	1
IC 214	0.11	-0.61	1.35	-9.56	0.66	5.08	1.82	7
NGC 3504	0.02	-0.56	1.45	-8.96	1
NGC 4194	0.00	-0.26	1.63	-8.99	1.24	6.81	1.13	1,7
NGC 2798	0.01	0.03	2.05	-9.01	1
NGC 3256	0.55	0.16	1.88	-8.36	1.23	5.48	0.47	1,7
NGC 7552	0.00	0.48	2.12	-8.44	1.29	6.11	0.1	1,3,7

relationship:

$$\langle \beta - \beta_{\text{SW}} \rangle = -0.16 \pm 0.04. \quad (2)$$

This was determined from measuring β of 16 high signal-to-noise IUE spectra with no noticeable SW/LW break, both with and without the tenth window. The uncertainty is the standard error on the mean.

The only non-UV quantity in Fig. 1 is the far-infrared flux F_{FIR} which is derived from *InfraRed Astronomical Satellite* (IRAS) 60 and 100 μm flux densities listed by NED and is defined by Helou et al. (1988). For convenience in notation we define the ratio $F_{\text{FIR}}/F_{1600} = \text{IRX}_{1600}$

3.2. Errors

Typical error bars are shown in the bottom right of fig 1. We estimate an uncertainty in β of 0.14 from the χ^2 fits to the spectra, and the scatter about the mean relationship given in eq. 2). We adopt an average uncertainty in F_{1600} of 5%, which we showed in Paper I is the typical level of agreement between broad band HST UV fluxes and IUE spectra. This is higher than expected from the error spectra presented with the Kinney et al. (1993) IUE atlas, which are commonly at the 10% – 20% level *per pixel*, and hence $< 1\%$ when integrated over the UV passband. The level of agreement between HST and IUE is worse probably because of the centering errors with IUE. The median uncertainty in F_{FIR} for our sample is 7%, derived from the uncertainties in F_{60} and F_{100} as listed by NED. Combining the F_{1600} and F_{FIR} errors we estimate that the error in $\log(F_{\text{FIR}}/F_{1600})$ is 0.04 dex.

These uncertainties represent random errors. Systematic errors will effectively move all data points with respect to the zeropoints of the axes. C. Robert (1999, private communication) estimates that there is a systematic uncertainty of 0.15 in β due to the placement of the continuum windows in the spectrum fit.

Figure 1 illustrates that the random errors in the quantities are smaller than the scatter about the relationship. Hence, the scatter in Fig. 1 is largely intrinsic. Possible sources of intrinsic scatter are dust geometry, dust composition, and intrinsic spectral slope (which depends on the star formation history), all of which may vary from galaxy to galaxy.

3.3. $\beta - A_{1600}$ calibration

We assume that F_{FIR} is due to the thermal emission of dust heated by the radiation it absorbs. This consists primarily of non-ionizing photons with the addition of Ly α photons which are resonantly scattered

by Hydrogen until they are absorbed by dust grains. We assume that ionizing photons do not significantly contribute to dust heating⁵. For these assumptions IRX_{1600} can be written as

$$\text{IRX}_{1600} = \frac{F_{\text{FIR}}}{F_{1600}} = \left(\frac{F_{\text{Ly}\alpha} + \int_{912\text{\AA}}^{\infty} f_{\lambda',0} (1 - 10^{-0.4A_{\lambda'}}) d\lambda'}{F_{1600,0} 10^{-0.4A_{1600}}} \right) \left(\frac{F_{\text{FIR}}}{F_{\text{bol}}} \right)_{\text{Dust}} \quad (3)$$

$f_{\lambda,0}$ is the unattenuated flux density of the emitted spectrum, A_{λ} is the net absorption in magnitudes by dust as a function of wavelength, and $F_{\text{Ly}\alpha}$ is the Ly α flux. In our models $F_{\text{Ly}\alpha}$ is derived from the spectrum shortward of 912 \AA using the standard assumption that each ionizing photon results in one recombination and consequent decay down to case-B population levels. Customarily one adopts a form of the absorption (or extinction) law scaled by the optical reddening, e.g. $A_{\lambda} = X_{\lambda} E(B - V)$. In eq. 3 the first term gives the bolometric flux of the absorbed radiation, normalized by F_{1600} , and the second term gives the fraction of the bolometric flux emitted by dust that is intercepted by the FIR passband (e.g. Helou et al. 1988).

Strictly speaking IRX_{1600} in our model depends on the intrinsic spectrum and the absorption curve, even at wavelengths well outside the 1600 \AA passband. However, for dust heating dominated by young stellar populations eq. 3 is well approximated by the formula

$$\text{IRX}_{1600} = (10^{0.4A_{1600}} - 1) \left(\frac{F_{\text{Ly}\alpha} + \int_{912\text{\AA}}^{\infty} f_{\lambda',0} d\lambda'}{F_{1600,0}} \right) \left(\frac{F_{\text{FIR}}}{F_{\text{bol}}} \right)_{\text{Dust}} \quad (4)$$

Here the first term gives the fraction of $F_{1600,0}$ that is absorbed by dust; the second term is similar to a bolometric correction, giving the maximum amount of heating available to the dust divided by the intrinsic 1600 \AA flux; and the third term is the same as the second term in eq. 3. The ratio of eqs. 3 and 4 asymptotes to unity as $A_{\lambda} \rightarrow \infty$ for all λ . We have calculated this ratio under a variety of assumptions applicable to starbursts. The constant star formation rate (CSFR) solar metallicity models of Leitherer and Heckman (1995) having a Salpeter (1955) IMF slope and durations of $\Delta t = 1$ to 100 Myr were used as the initial spectra. Leitherer and Heckman (1995) varied other parameters in their population models including metallicity, IMF slope and cutoff, and other star formation histories (i.e. instantaneous bursts). They find that as long as the population is ionizing (i.e. produces a strong ionizing flux, as expected for starbursts by their strong emission line spectra), these

⁵Starburst population models indicate that typically only $\leq 10\%$ of the bolometric luminosity of starbursts is emitted below 912 \AA (Leitherer & Heckman, 1995). The fraction of this that is directly absorbed by dust grains is estimated to be $\sim 25\%$ (Smith, Biermann, & Mezger 1978).

parameters have very little effect on the overall UV spectrum which has $\beta_0 = -2.0$ to -2.6 in all cases. This range in intrinsic β is well covered by the models we examine here. The absorption was parameterized by $E(B - V) = 0.01$ to 1 and a variety of forms of X_λ including the following extinction laws (assuming extinction = absorption): Galactic (Seaton, 1979), LMC (Howarth, 1983), and SMC (using a polynomial fit to the Bouchet et al. 1985 curve); and the starburst absorption laws of Kinney et al. (1994), Calzetti et al. (1994), and Calzetti et al. (1997). In all cases the ratio of equations 3 and 4 is within 30% of unity for $A_{1600} \gtrsim 0.3$ mag. We conclude that eq. 4 is a good approximation of IRX_{1600} when the dust is heated by intrinsically young stellar populations and as long as the form of X_λ is not extremely different from standard absorption/extinction laws.

Equation 4 can be rewritten as

$$IRX_{1600} = (10^{0.4A_{1600}} - 1)B, \quad (5)$$

where B is the ratio of the two bolometric like corrections:

$$B = \frac{BC(1600)_\star}{BC(FIR)_{Dust}}, \quad (6)$$

$$BC(1600)_\star = \left(\frac{F_{Ly\alpha} + \int_{912\text{\AA}}^{\infty} f_{\lambda',0} d\lambda'}{F_{1600,0}} \right)_\star \quad (7)$$

$$BC(FIR)_{dust} = \left(\frac{F_{bol}}{F_{FIR}} \right)_{Dust} \quad (8)$$

Here we assume that B is constant, and estimate the best value for it. We do this by cross comparing observations with models of the photometric properties of stellar populations ($BC(1600)_\star$) and dust emission ($BC(FIR)_{dust}$).

Values of $BC(1600)_\star$ were calculated for the CSFR population models of Leitherer & Heckman (1995) with standard Salpeter (1955) IMF slope, and an upper mass limit of $100 M_\odot$. For burst durations in the range of 0 to 100 Myr, we find $1.56 \leq BC(1600)_\star \leq 1.76$. We also calculated $BC(1600)_\star$ directly from the observed SED of NGC 1705, one of the least extincted sources in our local sample. We started with the observed IUE + optical SED published by Storchi-Bergmann et al. (1995) after correction for Galactic extinction. This was extended down to $\lambda = 912\text{\AA}$ by extrapolation using the power law fit (yielding $\beta = -2.40$). The SED was extended redwards to $\lambda = 2.4 \mu\text{m}$ using the *JHK* photometry of Jones as reported in Meurer et al. (1992)⁶. The total $H\alpha$ flux given by Meurer et al. (1992) was converted to $F_{Ly\alpha}$ assuming case B recombination. The integral in eq. 7 was evaluated directly from the SED, and

$F_{1600,0}$ was measured with SYNPHOT. This yields $BC(1600)_\star = 1.81$. Note that this may be a bit overestimated (by up to 20%) since there appears to be a break between the SW and LW portions of the IUE spectrum, with the SW portion being relatively underestimated. We conclude that within the uncertainties the NGC 1705 measurement is consistent with the model estimates.

The bolometric dust correction $BC(FIR)_{Dust}$ was estimated empirically by directly calculating $BC(FIR)_{Dust}$ for the ultra-luminous infrared galaxies observed in the FIR-submm by Rigopoulou, Lawrence, & Rowan-Robinson (1996). Two galaxies (Mrk 231 and IRAS05189-2524) were rejected from their sample because they have strong AGN emission. A smooth SED was drawn through the SED observations of the remaining sources and integrated over $1\mu\text{m} < \lambda < 1.0\text{mm}$ to determine F_{bol} . The individual $BC(FIR)_{Dust}$ measurements are shown in the top panel of Fig. 2, as a function of FIR color $f_\nu(60\mu\text{m})/f_\nu(100\mu\text{m})$. For comparison the FIR colors of local UV selected starbursts are shown in the bottom panel of Fig. 2. We find that six of the seven remaining galaxies in the Rigopoulou et al. sample have $\langle BC(FIR)_{Dust} \rangle = 1.47$ with a dispersion of 0.13. The seventh, 08572+3915 has $f_\nu(60\mu\text{m})/f_\nu(100\mu\text{m}) = 1.64$, much warmer than the majority of the UV selected starbursts, almost all of which have $0.3 < f_\nu(60\mu\text{m})/f_\nu(100\mu\text{m}) < 1.1$.

The top panel of Fig. 2 shows that the empirical $BC(FIR)_{Dust}$ measurements are in good agreement with Helou's et al. (1988) dust emission models. These models are very simple. They treat the dust distribution as emitting thermal radiation at a single temperature, with emissivity $\propto \nu^n$. We caution that more realistic modeling of interstellar dust emission includes multiple temperature emission with $n \approx 1$ to 2 (e.g. Désert, Boulanger, & Puget 1990). Figure 2 illustrates that single temperature models with $n \approx 1$ provide a good approximation to the dust emission of starbursts for the limited purpose of calculating $BC(FIR)_{Dust}$. Adopting this model we have calculated $BC(FIR)_{Dust}$ for the local UV selected starbursts, which tend to have somewhat cooler colors in the FIR than ultraluminous infrared galaxies. These have a median $BC(FIR)_{Dust} = 1.37$, with 80% of the sample having $1.36 \leq BC(FIR)_{Dust} \leq 1.44$.

We adopt $BC(1600)_\star = 1.66 \pm 0.15$, and $BC(FIR)_{Dust} = 1.4 \pm 0.2$, yielding $B = 1.19 \pm 0.20$. Here the "errors" actually indicate the amount of leeway allowed by our model calculations and limited measurements of starbursts, as described above.

⁶Their *I* band photometry was used to calculate a 0.34 mag aperture correction to match the IUE size aperture of Storchi-Bergmann et al. (1995).

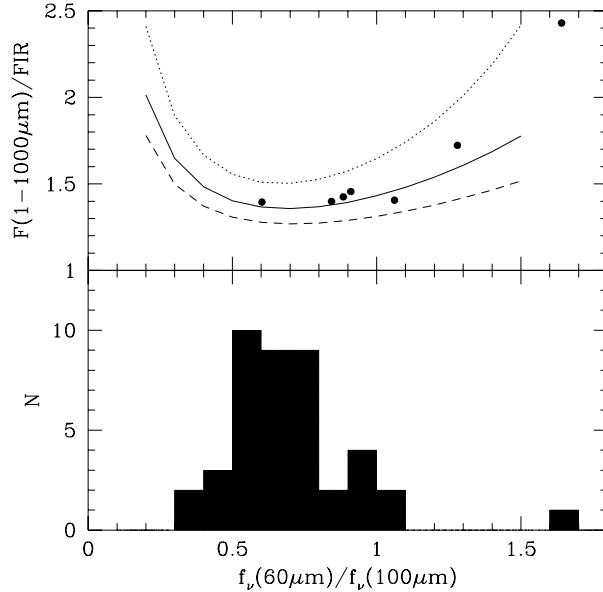


FIG. 2.— The top panel shows the dust bolometric correction $BC(FIR)_{\text{dust}}$ for the non-AGN ultra luminous infrared galaxies in the sample of Rigopoulou et al. (1996) plotted against FIR color. The dotted, solid, and dashed lines show the single temperature dust emission models of Helou et al. (1988), for emissivity indices $n = 0, 1,$ and 2 respectively. The bottom panel shows the distribution of FIR colors for local UV selected starbursts.

Equation 5 can now be written logarithmically as

$$\log(\text{IRX}_{1600}) = \log(10^{0.4A_{1600}} - 1) + \log B, \quad (9)$$

$$\log(\text{IRX}_{1600}) = \log(10^{0.4A_{1600}} - 1) + 0.076 \pm 0.044. \quad (10)$$

Here we see the beauty of the approximation eq. 4; it allows the direct transformation of IRX_{1600} to 1600\AA absorption as shown on the right hand side of Fig. 1.

Our adopted model for the $\text{IRX}_{1600} - \beta$ relationship is a simple linear fit of A_{1600} versus β . To first order this is what one would expect for absorption by a foreground screen of dust. The adopted fit, which is shown in Fig. 1, is

$$A_{1600} = 4.43 + 1.99\beta. \quad (11)$$

It was determined from separate unweighted least squares fits of A_{1600} versus β , and β versus A_{1600} , which were then averaged. The dispersion about this fit is 0.55 mag in A_{1600} , 0.28 in β and 0.30 dex in $\log(\text{IRX}_{1600})$ (the latter including only galaxies with $\beta > -2.23$). Consequently the standard error in the fit zeropoint is 0.08 mag in terms of A_{1600} and 0.04 in terms of β . Since the scatter about the fit is significantly larger than the errors, it is largely intrinsic. Hence, a more sophisticated fit (e.g. a full χ^2 fit with weighting by errors) will not improve the quality of the fit. Instead, improvement can only occur with an increase in sample size.

This fit implies the spectral slope in the absence of dust absorption is $\beta_0 = -2.23$. This result is consis-

tent with what is expected of naked ionizing populations, which Leitherer & Heckman (1995) show to have $\beta_0 = -2.0$ to -2.6 (cf. Paper I). In Table 2 the slope of the absorption law, $dA_{1600}/d\beta$ derived here is compared with other extinction and absorption laws. The slope we derive is in the middle of the range for the starburst absorption laws derived in other studies. In particular, it is between the values derived by Calzetti et al. (1994) and Calzetti (1997). Note that the Galactic extinction law has a very large slope because the 2175\AA absorption feature counteracts the reddening of β to a large degree.

3.4. Photometric versus spectroscopic β

In Paper II we derived the following relationship between β and $(V_{606} - I_{814})_{\text{AB}}$ color:

$$\beta_{\text{phot}} = 3.23(V_{606} - I_{814})_{\text{AB}} - 2, \quad (12)$$

where the color is in the “AB” system ($m_{\text{AB}} = -48.6 - 2.5 \log(f_\nu)$, where f_ν is the spectral flux density per frequency interval in units of $\text{erg cm}^{-2} \text{s}^{-1} \text{Hz}^{-1}$). This was derived from first principles using the central wavelengths of the F606W and F814W WFPC2 filters and assuming a featureless power law spectrum and negligible filter widths. However, the UV spectra of starbursts typically contain numerous absorption features of both stellar and interstellar origin (Kinney et al. 1993). Emission lines, even $\text{Ly}\alpha$, are typically weak in starburst galaxies (Kinney et al., 1993). While the spectroscopically

TABLE 2
1600Å ABSORPTION LAW SLOPES

law	type	$dA_{1600}/d\beta$	reference
Starburst	absorption	1.99	This work
Starburst	absorption	1.44	Kinney et al. (1994)
Starburst	absorption	1.97	Calzetti et al. (1994)
Starburst	absorption	2.30	Calzetti (1997)
Galactic	extinction	4.42	Seaton (1979)
LMC/30 Dor	extinction	1.45	Howarth (1983)
SMC	extinction	1.05	Bouchet et al. (1985)

defined β avoids the lines, broad band filters cannot. Since the concentration of lines is particularly strong for $1216 < \lambda < 1700\text{\AA}$ one may expect an artificial reddening of the photometric β at $z \approx 3$ when these features are redshifted into the middle of the F606W passband. In addition at $z \geq 2.8$, Ly α enters the F606W passband. The Lyman forest strongly suppresses the flux bluewards of Ly α in such high redshift objects, again reddening β_{phot} .

We have used IUE starburst spectra to quantify these effects and model the calibration between photometric and spectroscopic β . The spectra we use were selected (by eye) to have high S/N and no discernible break between LW and SW portion of spectrum. This resulted in a final sample of 15 galaxies, as indicated in Table 1; most of these were also used to calibrate the A_{1600} versus β fit. Their spectroscopic β were measured as described above. These spectra were redshifted over the range $2 \leq z \leq 4$. In order to adequately account for the F606W filter width, the spectrum blueward of Ly α was taken to be a pure power law (using the measured β) normalized to the mean flux density at $\lambda = 1483 \pm 50 \text{\AA}$, and attenuated by the Lyman series forest which was modeled following the algorithm of Madau (1995). The $(V_{606} - I_{814})$ colors were then measured using SYNPHOT, yielding β_{phot} . Figure 3 plots the difference between β_{phot} and the standard spectroscopic β as a function of z .

Our calibration of the $\beta_{\text{phot}} - \beta$ relationship is a quadratic polynomial fitted to the median points shown in Fig. 3:

$$\beta_{\text{phot}} - \beta = 3.22 - 2.66z + 0.545z^2. \quad (13)$$

The fit is a χ^2 fit where the errors were taken to be the mean difference between the median and the 16th and 84th percentiles for a given z . The fit has an rms dispersion of 0.06. The reduced χ^2 is 0.19, hence the model is adequate for the given amount of scatter. Combining this with eq. 12 yields:

$$\beta = 3.23(V_{606} - I_{814})_{\text{AB}} - 5.22 + 2.66z - 0.545z^2 \quad (14)$$

which is now on the same scale as the $\beta - A_{1600}$ calibration of eq. 11.

3.5. Absolute star formation rate

The transformation of UV luminosity to SFR is highly model dependent. Hence, for most of this paper the emphasis will be on luminosity rather than the SFR. However, for comparison to other studies and to get a feel for the physics behind the UV luminosity, it is often convenient to transform it to a SFR. Our transformation is based on the population models of Leitherer & Heckman (1995). We adopt a solar metallicity, continuous star formation history population of duration 100 Myr, and a Salpeter (1955) initial mass function (IMF) with mass limits of 0.1 to $100 M_{\odot}$. For these parameters a SFR of $1 M_{\odot} \text{ yr}^{-1}$ produces a 1600Å flux density of $7.86 \times 10^{27} \text{ erg s}^{-1} \text{ Hz}^{-1}$ ($9.19 \times 10^{39} \text{ erg s}^{-1} \text{ \AA}^{-1}$), and hence an absolute magnitude of -18.15 ABmag (-20.81 STmag); the equivalent bolometric flux corresponds to $6.4 \times 10^9 L_{\odot}$. For the same star formation history and IMF parameters, Bruzual & Charlot (1993) stellar population models produce 8% more flux at 1600Å (see also comparison in Paper I). Not only is the choice of the particular population model important in this calibration, so to are the parameters of the IMF and the adopted star formation history. For example, if the lower mass limit of the IMF is raised to $1 M_{\odot}$ then the luminosity increases by a factor of 2.55 for a given SFR; if the duration of star formation is decreased to 10 Myr (1 Myr), then the luminosity decreases by a factor of 1.53 (12.9).

4. APPLICATION TO U-DROPOUT GALAXIES IN THE HDF

4.1. Sample selection

The above calibrations were applied to a sample of F300W (U) dropouts selected from the HDF V2.0 catalog (Williams et al. 1996). We will compare the

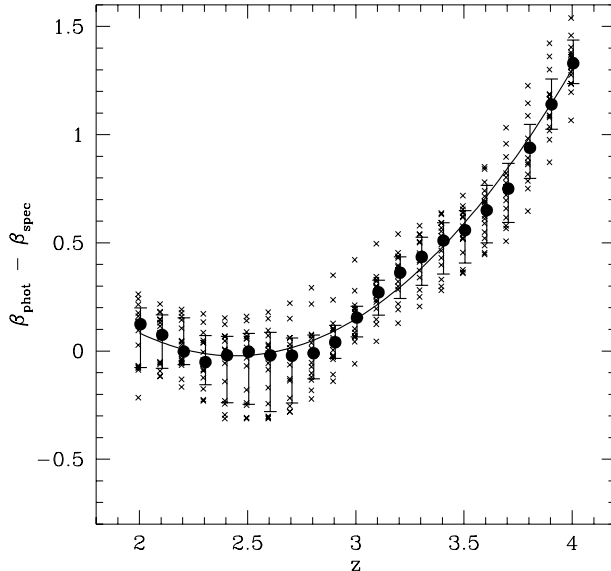


FIG. 3.— The difference between photometric and spectroscopic β plotted as a function of redshift. The \times marks indicate the individual measurements of the 15 template spectra. The circles represent the median of the measurements and the errorbars the 16th and 84th percentiles (i.e. $\approx 1\sigma$ errorbars). The solid line is the adopted polynomial calibration fit.

results from this sample to two other U -dropout samples extracted from the HDF by Madau and collaborators - in M96 and Madau et al. (1998; hereafter M98). M96 lays out all selection criteria in detail and lists all galaxies selected, and in addition it is the pioneering work in this field. M98 improves on M96 in several ways (see below). However, the results of M98 are model dependent, their U -dropout selection criteria are not explicitly given, and their final sample is not listed. Hence we adopt M96 as our primary comparison, and we model our sample selection on the criteria given therein.

Our sample selection differs from that of M96, primarily because we use $(V_{606} - I_{814})_{AB}$ rather than $(B_{450} - I_{814})_{AB}$ as a color selection criterion. This is done because for U -dropouts, the F450W filter is much more strongly affected by Ly α forest absorption than F606W. In our model, selecting by $(V_{606} - I_{814})_{AB}$ places a fairly strong limit on β and hence on A_{1600} . Figure 4 shows the $(V_{606} - I_{814})_{AB}$, $(U_{300} - B_{450})_{AB}$ two color diagram, and our selection box. Our selection criterion $(V_{606} - I_{814})_{AB} < 0.5$ was chosen to encompass the strong U -dropout plume but avoid relatively low- z interlopers. Our other selection criteria are virtually identical to M96; $(U_{300} - B_{450})_{AB} \geq 1.3$ is the crucial U -dropout selection criterion, while $B_{450} \leq 26.79$ ABmag is the magnitude limit⁷. Only sources in the WF chips are selected.

Another important difference with M96 is that their color selection box is not rectangular. They have an additional constraint $(U_{300} - B_{450})_{AB} > (B_{450} - I_{814})_{AB} + 1.2$, clipping the bottom right corner out of the box. This was introduced to avoid regions that model calculation indicate may be populated by low redshift galaxies. However, this corner, while relatively sparsely populated in the $(U_{300} - B_{450})_{AB}$ versus $(B_{450} - I_{814})_{AB}$ two color diagram, contains about $1/3$ the galaxies in the HDF with measured $2 < z < 4$ (Dickinson 1998). Since the clipped corner is red in $(B_{450} - I_{814})_{AB}$ the clipping biases against large A_{1600} . The color selection criteria of M98 are illustrated in Madau (1997), where they were revised in order to incorporate more galaxies with $2 < z < 4$. Less of the bottom right corner is clipped than in M96. We have opted for a rectangular selection box in order to minimize this bias and keep the color selection as simple as possible, and yet be very close to the M96 selection box. A total of 100 sources meet our selection criteria. These are listed in Table 3. Photometry for these galaxies can be found in Williams et al. (1996). In comparison M96 selected 69 U -dropouts, and Madau (1997) note that there are ~ 100 galaxies in their revised selection box. Dickinson (1998) using more robust photometry, a somewhat different color selection and a fainter limiting magnitude, isolates 187 U -dropouts in the HDF.

A small difference with M96 concerns how sub-

⁷Nominally, we have also adopted $V_{606} \leq 28.0$ ABmag in our selection. However, for our other selection criteria no objects approach this limit.

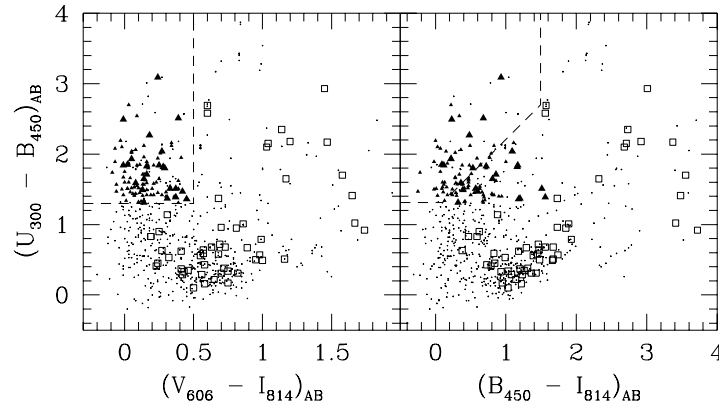


FIG. 4.— Two color diagrams of all objects (parents and daughters) in the HDF V2.0 catalog (Williams et al. 1996) with $B_{450} \leq 26.79$ ABmag. The dashed line in the left panel marks our adopted selection box for U -dropouts, while that in the right panel marks the selection box of M96. The symbol correspondence is as follows: large triangles - spectroscopically confirmed galaxies with $2 \leq z \leq 4$; squares - galaxies with spectroscopic $z < 2$; small triangles - other galaxies meeting our U -dropout selection criteria (i.e. they must be in the box at left); dots - other objects not meeting our selection criteria. Some of these latter objects are nevertheless in our selection box. However they do not pass our simple parent-daughter separation algorithm, and are not included (and hence are not highlighted) in order to avoid double-counting.

TABLE 3
LIST OF U -DROPOUTS SELECTED IN THE HDF

2-35.0	2-689.2	3-389.0	4-317.0
2-76.0	2-726.0	3-504.0	4-363.0
2-80.0	2-741.0	3-510.0	4-382.0
2-82.0	2-751.0	3-515.11	4-389.0
2-122.0	2-793.0	3-550.0	4-445.0
2-127.0	2-802.11112	3-593.0	4-488.0
2-239.0	2-822.0	3-633.1	4-491.0
2-321.2	2-824.0	3-674.0	4-497.0
2-373.0	2-889.0	3-677.0	4-555.1
2-381.12	2-890.0	3-736.0	4-557.0
2-392.0	2-901.0	3-748.0	4-576.0
2-449.0	2-903.0	3-813.0	4-588.0
2-454.0	2-916.0	3-875.0	4-590.0
2-456.12	2-949.0	3-902.0	4-599.0
2-456.22	2-973.11	3-916.0	4-602.0
2-525.0	3-41.0	4-52.0	4-639.0
2-547.0	3-83.0	4-83.0	4-660.0
2-565.0	3-118.0	4-85.2	4-676.0
2-585.1	3-126.0	4-96.0	4-681.0
2-591.0	3-221.2	4-109.0	4-724.11
2-594.0	3-243.0	4-194.0	4-825.0
2-604.1	3-286.0	4-252.0	4-858.0
2-637.0	3-296.1	4-274.0	4-878.1
2-643.0	3-321.2	4-289.0	4-926.2
2-689.11	3-335.0	4-316.0	4-936.0

structure is included. The HDF catalog lists objects found with the FOCAS software (Jarvis & Tyson 1981), which often splits a “parent” object into “daughters”. Both parents and daughters are listed in HDF V2.0. M96 carefully evaluate the image of each candidate U -dropout to determine whether it is likely to apply to the whole parent object or the daughter(s). Here, in cases where both daughter(s) and corresponding parent meet our selection criteria, only the parent object was included in our list of U -dropouts. This could cause the integrated 1600\AA luminosity density ρ_{1600} to be overestimated. This is because not all daughters need satisfy the U -dropout selection criteria for the parent to satisfy these same criteria. To estimate the maximum magnitude of this effect we considered the opposite extreme - when both parent and daughter(s) meet the selection criteria only the (lowest level) daughters that satisfy the selection criteria were included. This algorithm, results in ρ_{1600} being lower than our adopted sample by 16% (24% after absorption correction). This algorithm will underestimate ρ_{1600} because some daughters, having the right z to be selected as U -dropouts, will fail the magnitude limit, or because photometric errors (larger for the fainter daughters) may shift some daughters out of the color selection box. The ideal parent-daughter separation will, therefore, lie somewhere between these two extremes, and hence the effect on ρ_{1600} is likely to be a $\sim 10\%$ effect.

4.2. Application of calibration

The top panel of Figure 5 shows the color (β) absolute magnitude $M_{1600,0}$ of our HDF U -dropout sample. Here, β was calculated from the $(V_{606} - I_{814})_{\text{AB}}$ color listed in the HDF V2.0 catalog (Williams et al. 1996) using eq. 14; where z was taken from the compilation of Dickinson (1998) where possible, otherwise we adopt an average value $\langle z \rangle = 2.75$. This is the same U -dropout $\langle z \rangle$ adopted by M96, and very close to $\langle z \rangle = 2.74$ of the galaxies in our sample with measured z . The apparent AB magnitude at $\lambda = 1600\text{\AA}(1 + z)$ was interpolated between the V_{606} and the I_{814} magnitudes. This is effectively a k correction. The y axis shows the absolute AB magnitude at $\lambda_0 = 1600\text{\AA}$ corrected for UV absorption following eq. 11, while the broken diagonal lines indicate constant M_{1600} if there were no A_{1600} correction. The hatched region shows the region that is incomplete due to our selection criteria. The lower selection limit is slanted because of the A_{1600} correction and because of color terms in the k correction and in the translation of the B_{450} limiting magnitude into the V_{606} and I_{814} bands.

The middle panel of Fig. 5 shows the β distribution of the U -dropouts, while the bottom panel shows

that of the calibrating local sample for comparison. The color distribution of the local sample spans a larger range than the U -dropouts. The two-sided Kolmogorov-Smirnov test gives a 0.3% chance that the two distributions were randomly drawn from the same parent distribution. These differences are partially due to our $(V_{606} - I_{814})_{\text{AB}} < 0.5$ selection limit which corresponds to $\beta \lesssim -0.42$ for $z = 2.75$, or equivalently $A_{1600} \lesssim 3.6$ mag. The local sample has no specific β selection. If we apply a $\beta < -0.42$ limit to the local sample then the two-sided Kolmogorov-Smirnov test gives a 3% chance that the local and U -dropout sample were randomly drawn from the same parent distribution; i.e. the two samples are more similar when similar β selection criteria are applied. The U -dropout sample is *bluer* than the local sample having $\beta < -0.42$. The 20th percentile, median and 80th percentile of the U -dropout distribution are -1.9 , -1.6 , and -1.2 , while for the (β limited) local sample they are -1.8 , -1.4 , and -0.8 , respectively. One shouldn't read too much into this difference, in that the two samples were selected quite differently. The U -dropouts have well defined magnitude and color limits in the rest-frame UV while the local sample is composed of galaxies observed with IUE for a wide range of programs with heterogeneous initial selection criteria.

Luminosity functions at 1600\AA , ϕ_{1600} are shown for our U dropout sample in Fig. 6. Two cases are shown: with $(\phi_{1600,0})$ and without (ϕ_{1600}) the A_{1600} correction. The shape of ϕ_{1600} agrees well with that given by Dickinson (1998) for $M_{1600} \lesssim -19$ AB-mag. The drop-off in the last bin of our ϕ_{1600} is due to incompleteness. Dickinson's luminosity function extends further because of his superior photometric technique and consequent fainter limiting magnitude. Our luminosity function is 0.3 dex higher than that displayed by Dickinson because he renormalizes to match the luminosity function of U -dropouts selected from a larger ground based survey (Steidel et al. 1998). This factor of two difference probably reflects the field to field variation in ρ_{1600} .

The 1600\AA luminosity functions extend well beyond the range given for a sample of local UV selected galaxies by Buat & Burgarella (1998). Their luminosity function shows a distinct break at $L_{\text{bol}} \sim 10^{10} L_{\odot}$, corresponding to $M_{1600,0} = -18.7$ ABmag; a SFR of $4 M_{\odot} \text{ year}^{-1}$. The brightest galaxies in our U -dropout sample have $M_{1600} = -21.7$ ABmag, $M_{1600,0} = -24.1$, corresponding to a SFR of 19, 220 $M_{\odot} \text{ year}^{-1}$ with and without absorption correction, respectively. This is further confirmation of the assertion that U -dropouts are much more luminous than local UV selected starbursts. However, there are local starbursts with similarly high SFRs. These are the

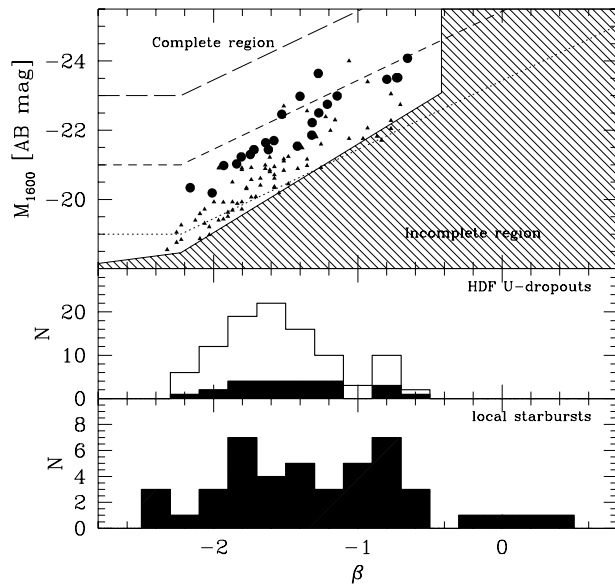


FIG. 5.— The top panel shows the UV color β versus absorption corrected absolute magnitude $M_{1600,0}$ diagram for our sample of U -dropouts. Large circles mark spectroscopically confirmed galaxies, while the rest of the U -dropouts are marked with triangles. The broken lines mark equal M_{1600} without dust absorption correction. The hatched region marks the incomplete region according to our selection criteria. The slanted boundary is calculated for galaxies at the limiting $B_{450} = 26.79$ ABmag with $z = 2.75$. It follows from eqs. 11 and 14 and relates the B_{450} limiting magnitude to the V_{606} and I_{814} bands using $(B_{450} - I_{814})_{\text{AB}} = 0.19 + 2.09(V_{606} - I_{814})_{\text{AB}}$, which was found using a linear least squares fit to the U -dropouts having $B_{450} \leq 26$ ABmag. The middle panel shows the β distribution of these galaxies. The solid histogram includes only the spectroscopically confirmed U -dropouts. For comparison the β distribution of the local starburst sample (from Fig. 1) is shown in the bottom panel.

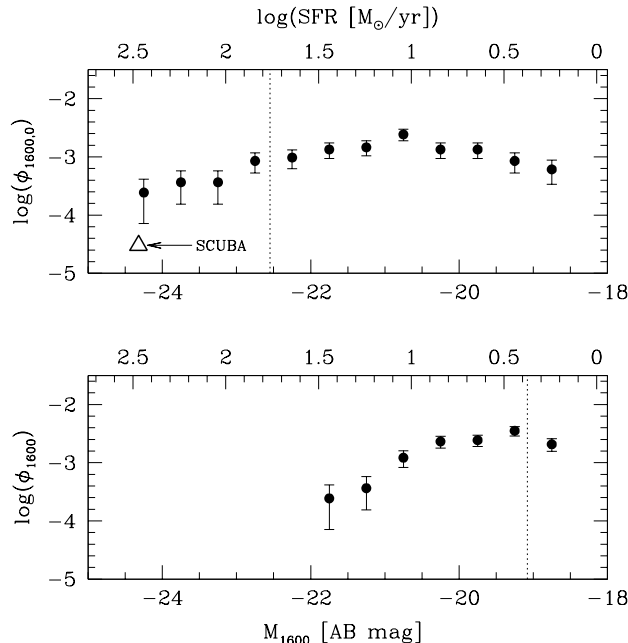


FIG. 6.— Luminosity function (ϕ) at $\lambda = 1600\text{\AA}$ of our sample of U -dropouts, with (top) and without dust absorption corrections. The error bars show the \sqrt{N} uncertainties. The dotted line shows the completeness limit. Data to the left of these lines are complete, to the right they are incomplete. The top axis of each plot converts M_{1600} to star formation rate. The units for ϕ are $\text{mag}^{-1} \text{Mpc}^{-3}$. The space density and luminosity of SCUBA sources, as estimated by Lilly et al. (1998), is indicated in the upper panel with a triangle.

ultra-luminous infrared galaxies (Sanders & Mirabel, 1997) which are selected in the far infrared.

From direct summation we derive the total absorption corrected UV luminosity of our selected U -dropouts to be $\Sigma L_{1600,0} = 3.8 \times 10^{34} \text{ erg s}^{-1}$. Assuming that the redshift range of $z = 2.0$ to 3.5 is uniformly sampled, then the volume containing the U -dropouts is $1.64 \times 10^4 \text{ Mpc}^3$ (M96), and the corresponding volume emissivity is $\rho_{1600,0} = 1.4 \pm 0.3 \times 10^{27} \text{ erg s}^{-1} \text{ Hz}^{-1} \text{ Mpc}^{-3}$ ($\rho_{\text{SFR}} = 0.18 \mathcal{M}_{\odot} \text{ yr}^{-1} \text{ Mpc}^{-3}$). The error quoted here is the quadratic sum of the zeropoint errors from equations 10, 11 and 14, and the sampling error determined from the bootstrap technique (e.g. Babu & Feigelson 1996). This $\rho_{1600,0}$ is actually a lower limit for the volume sampled by the HDF because we have made no completeness correction. This raises a difficult issue. The standard practice is to estimate the completeness from the luminosity function, without dust absorption. Doing so, Madau (1997) estimates a completeness correction factor of 1.45. Figures 5 and 6 show that in the presence of dust, the limiting $M_{1600,0}$ is not uniform. Rather it is much shallower for highly reddened galaxies than for lightly reddened sources. Hence the completeness correction could be higher. In addition there may be field to field differences in $\rho_{1600,0}$, due to large scale clustering. Such variations could be as high as a factor of 2 (Dickinson, 1998).

How accurate is our U -dropouts selection criteria for selecting high- z galaxies? Our sample includes all but three of the spectroscopically confirmed HDF galaxies with $z > 2$ as compiled by Dickinson (1998). The galaxy 1-54.0 was missed because it appeared on the PC1 chip rather than one of the WF chips; 3-512.0 has $z = 4.02$ and is B -dropout and hence too red to be a U -dropout; and 3-577.0 was not included because it is too faint for inclusion in our catalog. The remaining 23 spectroscopically confirmed high- z galaxies account for 47% of $\rho_{1600,0}$. We cross-checked our U -dropout selection against a list of all redshift measurements in the HDF (kindly made available by Mark Dickinson). None of our selection corresponds to galaxies with known $z < 2$. Dickinson (1998) notes a 90% success rate in finding high- z galaxies in the appropriate redshift range using the U -dropout technique on their ground based sample. While the photometric bands and selection criteria are somewhat different from ours, this suggests that the contribution of low- z interlopers to $\rho_{1600,0}$ should not be much higher than 10%.

4.3. The net effect of dust absorption

In this paper we are primarily interested in the effects of dust on the high- z UV emissivity. If

we calculate ΣL_{1600} and ρ_{1600} without correcting for dust absorption, the quantities are a factor of 5.4 ± 0.9 lower than the above estimates, e.g. $\rho_{1600} = 2.7 \pm 0.2 \times 10^{26} \text{ erg s}^{-1} \text{ Hz}^{-1} \text{ Mpc}^{-3}$. This is the net effect of dust absorption on *our sample* of U -dropouts. For comparison, M96 give $\rho_{1600} = 1.6 \times 10^{26} \text{ erg s}^{-1} \text{ Hz}^{-1} \text{ Mpc}^{-3}$ for their sample of U -dropouts. The samples are identical in their limiting magnitudes, so the difference in the uncorrected emissivities is due to the sample selection. In particular, Fig. 4 shows that the portion of ΣL_{1600} missing from the M96 sample is contained within the corner clipped from their otherwise rectangular color selection box. This corner contains preferentially reddened galaxies, hence this clipping biases against large A_{1600} . Relative to ρ_{1600} estimated by M96 our emissivity is a factor of 9.0 larger. We reiterate that the actual absorption-corrected $\rho_{1600,0}$ will be even higher than our estimates because we have not corrected for completeness, and we are not sensitive to galaxies having $A_{1600} > 3.6 \text{ mag}$.

More recently, Madau (1997) and M98 now estimate an uncorrected $\rho_{1600} = 2.6 \times 10^{26} \text{ erg s}^{-1} \text{ Hz}^{-1} \text{ Mpc}^{-3}$ for the volume sampled by the HDF U -dropouts, only 4% less than our estimate without dust correction. It is higher than in M96 because, as noted above, they adopt significant completeness corrections (a factor of 1.45) and use revised U -dropout selection criteria that clip less of the bottom-right corner in the $(U_{300} - B_{450})_{\text{AB}}$ vs. $(B_{450} - I_{814})_{\text{AB}}$ plane.

The 1600Å dust absorption factor, 5.4 ± 0.9 (equivalent to $A_{1600} = 1.8 \pm 0.2 \text{ mag}$), derived here for the U -dropouts is lower than our original estimate of a factor of 15 (Paper II), albeit within the factor of three uncertainty we originally estimated. Sawicki & Yee (1997) using the Calzetti (1997) absorption law, derived similarly high dust absorption factors of 15 to 20. Our new estimates are somewhat lower for a combination of reasons. Firstly, we now fit the $\text{IRX}_{1600} - \beta$ relation instead of adopting an absorption law (Calzetti et al. 1994) that is unconstrained by FIR data. Secondly, in Paper II we adopted the median absorption of the spectroscopically confirmed U -dropouts. Because of the $M_{1600,0} - \beta$ correlation (Fig. 5) this biases the net absorption. Finally, when deriving β from $(V_{606} - I_{814})_{\text{AB}}$ we now add a z dependent correction (eq. 14) to remove Lyman-forest and Lyman edge reddening, thus resulting in bluer colors and a smaller derived A_{1600} .

The uncertainty in our new estimate of the mean dust absorption factor of U -dropouts amounts to 16%, and includes zeropoint and sampling errors. It is likely to underestimate the true uncertainty since it does not include field to field variations. M98 and

Pettini et al. (1998) estimate 1500Å dust absorption factors of about three. Thus the difference between these groups and ours has narrowed considerably, and is probably within realistic errors on the dust absorption factor. However we reiterate our caution: 5.4 ± 0.9 represents a lower limit to the true mean 1600Å dust absorption factor of galaxies at $z \approx 3$. As discussed in §6.3, true 1600Å dust absorption factors on the order of 10 are still not ruled out.

Buat & Burgarella (1998) using a method very similar to ours, derive a somewhat lower mean absorption of 1.2 mag at $\lambda = 2000\text{Å}$ for a *local* sample of starbursts selected to be visible in both the UV and FIR. The difference probably is largely due to the lower luminosity of the galaxies in their sample, which has a median $L_{\text{bol}} \approx 10^9 L_{\odot}$ (SFR $\approx 0.16 M_{\odot} \text{ year}^{-1}$). The *U*-dropout sample has a median $L_{\text{bol}} = 8.5 \times 10^{10} L_{\odot}$ (SFR $\approx 13 M_{\odot} \text{ year}^{-1}$), nearly a factor of 100 higher. Because of the $M_{1600,0} - \beta$ correlation (Fig. 5), we expect the local sample to have a lower average amount of dust absorption (cf. Heckman et al. 1998).

In summary, our value for the dust absorption corrected UV emissivity $\rho_{1600,0} = 1.4 \times 10^{27} \text{ erg s}^{-1} \text{ Hz}^{-1} \text{ Mpc}^{-3}$ at $\langle z \rangle = 2.75$ is a factor of 9.0 higher than the uncorrected value given by M96 and a factor of 5.4 times higher than the uncorrected value given by M98. The increased UV emissivity relative to M96 is due to a combination of an improved *U*-dropout selection (factor of 1.7), and correction for dust absorption (factor of 5.4).

5. TESTS OF THE STARBURST HYPOTHESIS

Our determination of the UV opacity in high- z galaxies relies on the similarity of the *U*-dropouts to local starburst galaxies; the intrinsic SEDs of the two groups must be similar for our method to work. In §2 we reviewed how the overall spectral properties of the two samples are similar. Here we concentrate on recent observational studies of high- z galaxies that are especially relevant to estimating UV opacities.

5.1. Rest frame optical emission lines

If the high- z galaxies are intrinsically redder in the UV than local starbursts (i.e. $\beta_0 > -2.2$), then we would overestimate A_{1600} and hence $\rho_{1600,0}$. This could occur if the high- z galaxies are dominated by *older* stellar populations (which would have a larger z of formation) or, if for some reason, their stellar IMF were deficient in the highest mass stars. Rest-frame optical emission lines present an ideal test for this hypothesis. Starbursts are by nature dominated by highly ionizing populations. Indeed the calibrating IUE sample used in §3 were classified as starbursts primarily by the presence of intense narrow optical emission lines, arising in the ionized medium

surrounding the starbursts. Hence, the ratio of line flux to flux density f_{1600} is a measure of the color from below the Lyman-limit to 1600Å, modulated by dust absorption.

For $z = 2 - 3.5$ rest-frame optical emission lines are redshifted into the observed-frame near infrared. With careful, and very long exposures, the brightest optical lines are detectable in the brightest *U*-dropout galaxies with four meter class telescopes. Detections and fluxes have been reported by several groups including Pettini et al. (1998), Wright & Pettini (1998), Bechtold et al. (1997), and Bechtold et al. (1998). The detections correspond to *U*-dropouts discovered from the ground or in the HDF, as well as other sources that meet the photometric criteria for being *U*-dropouts. Figure 7 shows the line fluxes of these sources normalized by the rest frame 1600 Å flux density f_{1600} of the sources compared to β . Both f_{1600} and β were estimated from published photometry, where possible (otherwise from published spectra). The pseudo-equivalent widths $F(\text{line})/f_{1600}$ have been corrected for Galactic extinction and cosmological stretching only. No attempt has been made to correct for internal absorption. Results for three different lines are shown - H β , H α , and [O III] 5007Å. In cases where the [O III] 4959Å line was detected, it was multiplied by 3.0 to convert it to an [O III] 5007Å flux. A sample of local starburst galaxies observed by Storchi-Bergmann et al. (1995) and McQuade, Calzetti, & Kinney (1995) is shown for comparison. The relevant data is listed in Table 1. This UV selected sample has a high degree of overlap with the sample used in §3.

Figure 7 shows that the detected *U*-dropouts have line flux to UV flux density ratios consistent with local starburst galaxies. The one exception is the H α observation of the lensed galaxy MS1512-cB58 by Bechtold et al. (1997). Wright & Pettini (1998) have also detected this galaxy in H β emission, and the corresponding H β pseudo-equivalent width is well within the scatter of points for local starbursts as shown in the bottom panel of Fig 7. The discrepancy between the H α and H β measurements may be due to the lensed nature of the source, or perhaps may reflect the difficulty of the H α observations which were obtained at $\lambda = 2.443 \mu\text{m}$, the edge of the *K* band window. At this stage, none of the groups report non-detections in emission lines of known *U*-dropouts. We conclude that *U*-dropouts are ionizing sources to the same degree as local starbursts, and hence do not have an intrinsically redder continuum than the local sample.

5.2. Far infrared and radio continuum observations

If there is significant UV extinction of galaxies at $z \approx 3$, then perhaps the dust can be detected directly

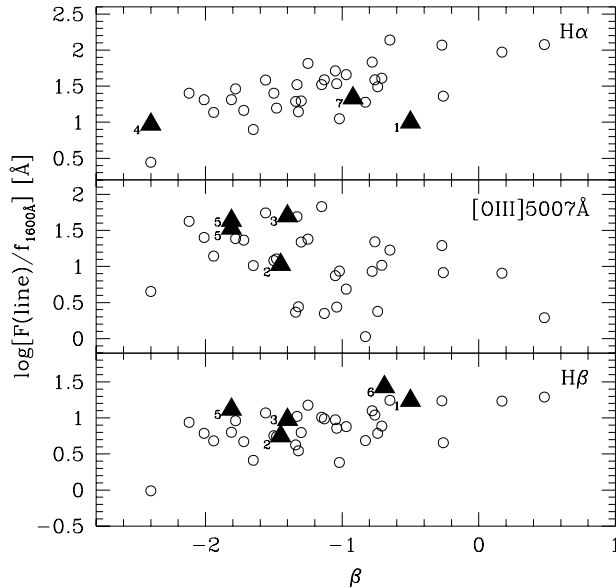


FIG. 7.— Line flux to UV flux density ratio compared to UV spectral slope. The open circles show a local sample of UV selected starbursts, using data originally published by Storchi-Bergman et al. (1995) and McQuade et al. (1995). The labelled triangles represent seven U -dropouts observed by Pettini et al. (1998), Wright & Pettini (1998); Bechtold et al. (1997) and Bechtold et al. (1998). The label - galaxy name correspondence is (1) MS1512-cB58; (2) Q0000-D6; (3) Q0201-C6; (4) Q0201-B13; (5) B2 0902-C6; (6) DSF 2237a-C2; and (7) A2218-A384. These data have been corrected for the redshift stretching of the spectral energy distribution.

in the rest frame FIR or indirectly in the radio via the radio-FIR correlation (Helou 1991). Two groups have recently claimed (marginal) detections of sources in and near the HDF in these wavelength regimes some of which which they attribute to $z \approx 3$ star forming galaxies. Here we show that the number and fluxes of these marginal detections are consistent with the expectations of our dust absorption model.

The sub-mm regime, corresponding to the rest frame FIR, is a promising window to look for high- z galaxies since the “negative k -corrections” for dust emission can cancel out the effects of fade-out with distance, making dusty galaxies easier to detect with increasing z (Guiderdoni et al. 1997). Several groups have now obtained deep sub-mm imaging with SCUBA⁸ on the 15m JCMT⁹ (e.g. Smail, Ivison & Blain, 1997; Barger et al. 1998; Eales et al. 1998; Hughes et al. 1998; Lilly et al. 1998). All report 850 μ m detections at the mJy level that they largely attribute to galaxies having $z > 1$. Indeed one of the SCUBA detections, SMM02399-0136, has a clear optical counter-part and spectroscopic determination of $z = 2.8$ (Ivison et al. 1998). However, Lilly et al. (1998) note that a sizable fraction of these sources may have $z < 1$. Furthermore, the emission line spectrum of SMM02399-0136 is indicative of a Seyfert 2 galaxy, cautioning us that not all of the dust seen by

SCUBA need be warmed by star-formation alone.

The study of Hughes et al. (1998) is particularly relevant because it is of a field centered on the HDF. They report five sources above their detection limit of 2mJy. Since this limit is set by source confusion (beam FWHM $\approx 15''$), none of their optical identifications is totally secure. They attempt to improve the accuracy of their identifications using photometry, including photometric redshifts. They claim that 4/5 of their detections are best identified with sources having $z \gtrsim 2$. The brightest of these has $f_{850\mu\text{m}} = 7 \pm 2$ mJy.

In Table 4 we present $f_{850\mu\text{m}}$ estimates for HDF U -dropouts based on our dust absorption model, and the optical photometry of Williams et al. (1996). To do this we used eqns. 10 and 11 to estimate the rest frame F_{FIR} from the rest frame F_{1600} and β estimates. F_{FIR} was then converted to $f_{850\mu\text{m}}$ using the FIR SED of the prototypical IR luminous starburst Arp 220 as modeled by a spline fit through the the measurements of Rigopoulou et al. (1996) and Klaas et al. (1997). Only the galaxies with the brightest predicted $f_{850\mu\text{m}}$ values are listed. The table is arranged in order of decreasing predicted $f_{850\mu\text{m}}$. The corresponding rest frame 1600 \AA flux densities (uncorrected for dust absorption) do not come out to be similarly sorted. This is because it is the dust reprocessed flux that is im-

⁸Sub-mm Common User Bolometer Array

⁹James Clerk Maxwell Telescope

portant. Since our adopted U -dropout sample is color limited (i.e. $A_{1600} \lesssim 3.6$ mag), the brightest predicted infrared fluxes correspond to the brightest and reddest U -dropouts. The UV absorption A_{1600} listed in this table is calculated from the $(V_{606} - I_{814})_{AB}$ as outlined in §3.3.

None of these galaxies have predicted $f_{850\mu\text{m}} > 2$ mJy, consistent with the fact that none were detected by Hughes et al.. Likewise, none of the claimed optical counterparts of $f_{850\mu\text{m}}$ detections meet our criteria of being U -dropouts. One is clearly a $z \approx 1$ galaxy. Three are fainter than our adopted inclusion limit. The remaining galaxy HDF850.3 is in the PC1 chip and identified as 1-34.2. Its $(V_{606} - I_{814})_{AB} = 0.33$ is within our selection limits, but its $(U_{300} - B_{450})_{AB} = 1.08$ color is marginally too blue to be considered a U -dropout, but consistent with a photometric $z \approx 1.95$ estimated by Mobasher et al. (1996).

The non-intersection of our U -dropout catalogue and the $850\mu\text{m}$ sample of Hughes et al. suggests that the sub-mm detections correspond to infrared luminous starbursts or AGN that are so dust enshrouded that they are not selected as U -dropouts either because they are too extinguished and/or because they are too reddened. The Hughes et al. identification of two $850\mu\text{m}$ sources (HDF850.1, HDF850.2) with fairly blue galaxies ($(V_{606} - I_{814})_{AB} < 0.5$) also suggests that the β -IRX $_{1600}$ calibration breaks down for heavily extinguished infrared-luminous starbursts. Further work is needed to confirm these identifications and secure reliable redshifts.

The remarkably tight radio - FIR correlation (Helou 1991) provides an indirect means to probe the FIR emission, and hence dust emission of starbursts. It is best defined at $\nu = 1.4$ GHz (21cm; e.g. Sanders & Mirabel, 1997). The radio emission of a wide range of star forming galaxies, including starbursts, is dominated by synchrotron emission at this frequency and up to ~ 30 GHz. Hence the correlation can be used to infer FIR fluxes from radio observations down to rest wavelengths of about 1 cm. Do we expect this correlation to hold at high- z ? Inverse Compton scattering from cosmic microwave background photons provides an alternative mechanism to synchrotron emission for cooling the relativistic electrons. The energy density of these photons will scale as $(1+z)^4$. However it is the total energy density of photons that is important for inverse Compton cooling. Even at $z \approx 3$ the energy density of cosmic microwave background photons will be an order of magnitude lower than internally produced energy density of starbursts having typical bolometric surface brightnesses of $S_e = 3 \times 10^{10} L_{\odot} \text{ kpc}^{-2}$ (e.g. Paper II) at $z = 3$. Since synchrotron emission clearly occurs in the face of intense internally pro-

duced emission in low- z galaxies, it does not seem likely that inverse Compton cooling will quench it for high- z galaxies where the total energy density is only marginally higher.

Richards et al. (1998) present a deep imaging survey of the HDF and surrounding areas obtained with the VLA at 3.5 cm ($\nu = 8.46$ GHz). Their 5σ detection limit is $9 \mu\text{Jy}$, and their 3.5σ marginal detection limit corresponds to $6.3 \mu\text{Jy}$. They marginally detect two HDF U -dropouts, 4-52.0 and 2-449.0 as listed in the HDF V2.0 catalog. While the detections are provisional, Richards et al. are confident that they are not spurious because they also are detected in a 1.4 GHz image of the HDF.

The logarithmic ratio of f_{ν} flux densities in the rest frame radio (1cm = 30 GHz) and UV ($1600\text{\AA} = 1.9$ PHz) and can be written as:

$$\log \left(\frac{f_{1\text{cm}}}{f_{1600\text{\AA}}} \right) = 2.78 - q_{\nu}(1\text{cm}) - \log(10^{0.4A_{1600}} - 1), \quad (15)$$

where q_{ν} is the radio-FIR logarithmic ratio:

$$q_{\nu} = \log \left\{ \frac{F_{\text{FIR}}[10^{-23} \text{ erg cm}^{-2} \text{ s}^{-1}]}{3.75 \times 10^{12} [\text{Hz}]} \bigg/ f_{\nu}[\text{Jy}] \right\}. \quad (16)$$

At $\lambda = 21$ cm, $q_{\nu}(21\text{cm}) = 2.35$ (Sanders & Mirabel, 1997). Since starbursts typically have radio spectral slopes $\alpha \approx -0.7$ (where $f_{\nu} \propto \nu^{\alpha}$), we expect $q_{\nu}(1\text{cm}) = 3.26$. For the prototypical starburst galaxy M82, $q_{\nu}(1\text{cm}) = 3.16$ is derived from the data listed by Carlstrom & Kronberg (1991). This is somewhat lower than expectations because free-free emission is starting to make a contribution to the 1cm flux of M82 (Carlstrom & Kronberg 1991). We adopt a rest frame $q_{\nu}(1\text{cm}) = 3.2$ and calculate the expected f_{ν} at 3.5cm ($f_{3.5\text{cm}}$) of the U -dropouts in our HDF sample using the above formulation, and modest (factor of a few at most) “ k ” corrections to transfer from the rest frame wavelengths of 1600\AA and 1cm, and the observed frame I_{814} and $\lambda = 3.5$ cm observations. Table 4 lists the results of these calculations for the expected 10 sub-mm brightest U -dropouts. Note that the f_{ν} ranking of the radio predictions is different from that of the FIR predictions. This is because the k corrections in the two wavelength regimes work in opposite direction with redshift at $z \approx 3$.

The sources in Table 4 include the two detections of Richards et al. (1998). Note that all of the galaxies in this table have predicted $f_{3.5\text{cm}}$ below the formal detection limits of Richards et al.. However the top five $f_{3.5\text{cm}}$ estimates are not far below their marginal detection limit, and include these two sources. In such cases we expect the fortuitous coincidences of uncertainties to allow some positive detections. These un-

TABLE 4
HDF U -DROPOUT FIR AND RADIO FLUX PREDICTIONS

Name	z	I_{814} [ABmag]	β	λ : A_{1600} [mag]	$(z+1)1600\text{\AA}$ Observed f_ν [μJy]	850 μm Predicted f_ν [mJy]	3.5cm Predicted f_ν [μJy]	3.5cm Observed f_ν [μJy]
4-52.0 ^a	2.931	24.06	-0.66	3.05	0.63	1.8	3.7	6.3 ± 2.6
4-878.1	(2.75)	23.28	-1.06	2.32	1.35	1.6	3.7	...
4-639.0	2.591	24.16	-0.73	2.92	0.52	1.1	2.8	...
2-585.1	2.002	23.50	-0.73	2.93	0.76	1.1	4.7	...
4-555.1	2.803	23.33	-1.27	1.93	1.39	1.1	2.3	...
4-445.0	2.268	23.75	-0.80	2.79	0.69	1.0	3.5	...
4-382.0	(2.75)	24.10	-0.95	2.52	0.61	0.9	2.2	...
2-127.0	(2.75)	24.72	-0.79	2.81	0.33	0.7	1.6	...
2-449.0 ^b	2.008	23.42	-1.14	2.17	1.01	0.6	2.7	7.0 ± 2.0
4-858.0	3.216	24.06	-1.40	1.70	0.78	0.6	1.0	...

^aSource 3647+1255 in Richards et al. (1998)

^bSource 3648+1416 in Richards et al. (1998)

certainties include the measurement bias mentioned above, the flux uncertainties listed by Richards et al. (~ 0.1 dex uncertainty), the intrinsic scatter about the radio-FIR relationship (~ 0.3 dex uncertainty; Devoreaux & Eales 1989), and the random scatter about the A_{1600} versus β fit (~ 0.1 dex uncertainty). The total random uncertainty is ~ 0.3 dex or a factor of ~ 2 . Hence random errors alone can account for the difference in the predicted and observed $f_{3.5\text{cm}}$ in the two galaxies detected by Richards et al.. Why aren't these galaxies also detected in the rest frame FIR? Scaling our predictions by the $f_{3.5\text{cm}}$ observed by Richards et al., we then expect $f_{850\mu\text{m}} = 3.2 \pm 1.3, 1.6 \pm 0.5$ mJy for 4-52.0 and 2-449.0 respectively. The latter is below the Hughes et al. detection limit, while the former is above it but by less than the flux uncertainty, and so could easily be missed. We conclude that the Richards et al. radio detections are consistent with the Hughes et al. SCUBA non-detections.

Our calculations show that U -dropouts in the HDF are just at the detection limit of state of the art deep rest frame FIR and radio observations. Somewhat deeper observations in these bands of either the HDF or other fields containing U -dropouts (preferably the brightest and reddest ones) have the potential for directly testing the β - IRX₁₆₀₀ relationship and verifying the existence of the radio-FIR correlation at $z \approx 3$. Hence they could be used to directly test the form of the UV absorption law. For example, the SMC law absorption model adopted by Pettini et al. (1997) would predict $f_{850\mu\text{m}} < 0.4$ mJy, and $f_{3.5\text{cm}} < 1\mu\text{Jy}$ for all the U -dropouts in our sample. Hence mJy level imaging at 850 μm and μJy level radio continuum imaging should detect the brightest

U -dropouts if our absorption model is correct, but would not detect any if lightly absorbed models were correct.

6. DISCUSSION

6.1. Color-luminosity correlation

The color-magnitude diagram of HDF U -dropouts, Fig. 5, shows that the highest luminosity galaxies, with or without A_{1600} correction, tend to be red. Similarly the bluest galaxies tend to have the lowest luminosity. That is, there is a color-luminosity correlation (also noted by Dickinson, 1998, private communications). The β - luminosity correlation is similar to that seen in local starburst galaxies (Heckman et al. 1998). As is the case for local starbursts, this correlation is not solely due to selection effects. While Fig. 5 clearly shows that we select against low-luminosity red U -dropouts, there is no selection against high luminosity very blue objects. The more luminous starbursts have a higher dust content. Presumably, dust content is related to metallicity. This is certainly born out for local starbursts where [O/H] correlates with β (Heckman et al. 1998). From Paper II, we know that the U -dropouts have similar surface brightnesses, hence the most luminous ones are the largest, and presumably the most massive galaxies. Putting these together implies a mass-metallicity relationship for U -dropouts like that seen in starburst (Heckman et al. 1998) and normal galaxies in the local universe. The presence of dust in the most luminous U -dropouts implies that they were previously enriched with metals. Hence we are not seeing the most luminous galaxies at the instant they "turn on". Their first generation of star formation must have oc-

curred at $z \geq 2.75$.

6.2. Optical line to UV continuum ratios as reddening indicators

Figure 7 illustrates the (un) usefulness of line to UV continuum ratios as indicators of dust absorption; the y axis is proportional to the ratio of the SFRs one would derive from emission lines and the UV continuum respectively, in the absence of dust absorption. Pettini et al. (1998) argue that the similarity of the SFR derived from $H\beta$ fluxes and the UV continuum indicates that dust absorption is not extreme. However, Fig. 7 shows little correlation between $F_{H\beta}/f_{1600}$ with β . In local starburst systems, we know that β is a good dust absorption indicator (Fig. 1); apparently $F_{H\beta}/f_{1600}$ is not. The only ratio that noticeably correlates (positively) with β is $F_{H\alpha}/f_{1600}$. However, the slope of the correlation is about half that expected by application of the LMC extinction law. The $F_{[OIII]}/f_{1600}$ ratio even shows an anti-correlation with β . This is probably due to the correlation of $[O/H]$ with β found for starbursts (Heckman et al., 1998) – highly reddened starbursts have higher metallicities, lower electron temperatures in the ionized medium, and hence lower $[OIII]/H\beta$ ratios than low reddening starbursts.

The $F_{H\alpha}/f_{1600}$ and $F_{H\beta}/f_{1600}$ results illustrate a result that is often overlooked: the dust absorption estimated from continuum observations is usually less than that estimated from HII emission. This was first noted by Fanelli, O’Connell, & Thuan (1988) and subsequently confirmed by others including Mas-Hesse, Arnault, & Kunth (1989), and Calzetti et al. (1994). The lack of correlation between $F_{H\beta}/f_{1600}$ and β indicates that the effective extinction law of starbursts is such that $A_{1600}(\text{continuum}) \approx A_{H\beta}(\text{HII})$. While uncorrected UV continuum fluxes and $H\beta$ line fluxes may imply the same SFRs, both are affected by similar amounts of dust absorption. Hence, emission line flux to UV continuum ratios do not provide strong constraints on dust absorption.

6.3. SCUBA detections and the nature of U -dropouts

The SFR of the various SCUBA detections is typically derived to be $> 100 M_{\odot} \text{ yr}^{-1}$ (e.g. Lilly et al. 1998). As shown in Fig. 6, this is consistent with the SFR derived for the brightest and reddest U -dropouts, after dust absorption correction. Such high values for the SFR are unprecedented for local UV selected starbursts, and typically only seen in FIR selected starbursts such as Arp220. This suggests that the most luminous starbursts at $z \approx 3$ are less dust enshrouded than those seen locally - the ultra-

luminous infrared galaxies. However, this conjecture is difficult to test, since there are very few UV observations of ultra-luminous infrared galaxies (cf. Trentham et al. 1999), hence the amount of UV absorption they suffer has not been properly characterized. Also shown in Fig. 6 is Lilly’s et al. (1998) estimate of the number density of the SCUBA sources in the redshift range $2 < z < 3$. This is also in fair agreement with the number density of the U -dropouts having the same luminosity. This comparison suggests that the SCUBA sources may be largely U -dropouts with modest amounts of dust absorption, rather than being completely opaque in the UV. Furthermore, it suggests that much of the SFR density at $z \approx 3$ can be recovered from rest-frame UV measurements alone.

Working against this suggestion is the fact that none of the HDF SCUBA sources detected by Hughes et al. (1998) correspond to known U -dropouts. However, the numbers are small, and the association with optical galaxies is still not secure. Hughes et al. estimate $\rho_{\text{SFR}} \approx 0.11 M_{\odot} \text{ yr}^{-1} \text{ Mpc}^{-3}$ at $z \approx 3$ from their SCUBA detections which is about half of the ρ_{SFR} we derive. This is only \sim five times larger than the M96 estimate (~ 3 times higher than the M98 estimate). Like us they do not extrapolate the luminosity function of their detections, hence the ρ_{SFR} is a lower limit consistent with our estimates. Alternatively, if the SCUBA sources are at $z \approx 3$ and a non-intersecting set with respect to U -dropouts (as suggested by the Hughes et al. identifications), then the sum of the Hughes et al. ρ_{SFR} and that derived from our U -dropout sample provides an improved lower limit: $\rho_{\text{SFR}} \gtrsim 0.30 M_{\odot} \text{ yr}^{-1} \text{ Mpc}^{-3}$ at $z \approx 3$ which is a factor $\gtrsim 15$ larger than that estimated by M96, and $\gtrsim 9$ times the uncorrected value estimated by M98.

M98 argue against such a high value of ρ_{SFR} since it would over-produce low mass stars in the present universe if it went on for more than about one Gyr. However, this argument assumes that the Lyman-dropouts have an IMF with constant Salpeter (1955) slope over the mass range of 0.1 to $125 M_{\odot}$. Recent observations of local starbursts suggest that their IMF is deficient in stars less massive than $3 M_{\odot}$ with respect to the Salpeter IMF (Nota et al. 1998; Siriani et al. 1999)

Since ρ_{SFR} is very model dependent, a more robust prediction of interest is the lower limit to the FIR emissivity. Summing the predicted FIR fluxes of all the HDF U -dropouts (using eq. 10) and normalizing by the volume yields $\rho_{\text{FIR}} > 7.2 \times 10^{29} \text{ erg s}^{-1} \text{ Hz}^{-1} \text{ Mpc}^{-3}$ at $z = 2.75$ evaluated at a rest wavelength of $80 \mu\text{m}$. If the SCUBA detections are too reddened or dimmed to be selected as U -dropouts then we can add them to our sample to get an improved lower limit: $\rho_{\text{FIR}} > 12 \times$

$10^{29} \text{ erg s}^{-1} \text{ Hz}^{-1} \text{ Mpc}^{-3}$. These are still lower limits because completeness corrections have not been made. These predictions can be tested directly with improved FIR, sub-mm, and radio observations (e.g. with the upcoming Sub-mm Array, and the SIRTf, FIRST, and PLANCK space missions).

6.4. Application to other redshifts

Our calibration of UV extinction is readily adapted to observations at redshifts other than $z \approx 3$ and hence other spectral domains. The main requirement is that the data include fluxes in two broad bands or coarse spectra covering the rest frame UV. Redshift information is also helpful, and that can be obtained photometrically to adequate accuracy from complementary rest frame optical - near IR data (e.g. from the Sloan Digital Sky Survey, or deep pointed observations). For example, serendipitous detections of galaxies with $z \gtrsim 5$ (e.g. Franx et al. 1997; Dey et al. 1998) indicate that galaxy formation had commenced by this epoch. One of these galaxies is a lensed arc at $z = 4.92$, whose broad band (observed frame) optical - near IR photometry yield $\beta = -1.63$ (Soifer et al. 1998), implying $A_{1600} \approx 1.2$ mag. Upcoming all sky surveys in the UV by GALEX (Martin et al. 1997) and TAUVEV (Brosch, et al. 1994) will probe the cosmological UV emissivity to $z \lesssim 2$. Extending deep imaging with the HST into the near IR with NICMOS allows Lyman edge systems to be detected out to $z \approx 8$ (I_{814} -dropouts).

There are a few caveats to using our methods, especially at low- z . Firstly, it is based on the assumption that the UV emissivity is dominated by starbursts. Possible contaminants are normal disk galaxies and old stellar populations. Ideally we want to include the UV light from normal disk galaxies when estimating star SFRs. The problem is that it is not known whether normal disks follow the starburst reddening law derived here. Their cool and warm ISM is dominated by a disk morphology, while starbursts typically have significant quantities of extra-planar ISM ejected by galactic winds (Heckman, Armus, & Miley 1990). In Paper I we suggested that winds shape the ISM around starbursts into a foreground screen, thus producing the $\text{IRX}_{1600} - \beta$ correlation. Further work has to be done to determine if normal disks have a reddening - UV absorption relation and to calibrate it. Fortunately normal disk and starburst galaxies can be distinguished in the UV by effective surface brightness (Paper II). Cosmological surface brightness dimming renders normal spiral galaxies difficult to detect by $z \approx 3$ (Giavalisco et al. 1996; Hibbard & Vacca, 1997), hence they do not contaminate the U -

dropout sample. Old stellar populations produce significant UV “upturn” emission. If they significantly contaminate a UV survey then the assumption that UV light is due to recent star formation is seriously compromised. Old stellar populations can be distinguished and removed from UV surveys by extending the broad-band SED into the rest frame optical.

Secondly, our technique has been calibrated to a fairly modest $A_{1600} \approx 5$ mag (Fig. 1). While the local calibrating sample contains several well known dusty starbursts (e.g. NGC 1614, NGC 3504, NGC 3256, NGC 7552), it doesn’t contain any of the “Ultra-Luminous Infrared Galaxies” (ULIRGs) which are the most luminous starbursts known (Sanders & Mirabel, 1997). It is not known if they fall on or continue the $\text{IRX}_{1600} - \beta$ relationship since the number of these galaxies observed in the UV is rather meager (Trentham et al. 1999). The amount of totally obscured star formation in the local universe can be estimated by applying our absorption algorithm to a blind UV survey such as will be produced by GALEX, after correction for contaminants as suggested above. This will yield an estimate of $\rho_{1600,0}$ and also the corresponding density of UV flux processed to the FIR. Comparison with ρ_{FIR} derived from IRAS, ISO¹⁰, or SIRTf¹¹ observations will yield the fraction of completely buried star formation.

7. SUMMARY

The strong similarity between local starburst galaxies and Lyman limit systems at $z \approx 3$ provides a strong impetus to use starbursts as templates for interpreting the properties of high- z galaxies. The fact that starburst galaxies redden as more of their UV light is absorbed by dust is demonstrated by a strong correlation between their FIR to UV flux ratios and their ultraviolet spectral slopes β (color). Our A_{1600} versus β calibration is a simple empirical fit to this correlation. Hence, by design it recovers the UV light that has been reprocessed to the FIR.

We applied this calibration to a U -dropout sample selected from the HDF V2.0 catalog. This sample has an identical limiting mag to that of Madau et al. (1996: M96). However, the color selection is somewhat different, resulting in a fairly uniform limiting $A_{1600} \lesssim 3.4$ mag. In contrast the M96 U -dropout sample has a non-uniform bias against large A_{1600} . For our adopted cosmological parameters of $H_0 = 50 \text{ km s}^{-1} \text{ Mpc}^{-1}$, $q_0 = 0.5$, the rest-frame comoving UV emissivity of our sample is $\rho_{1600} = 2.7 \times 10^{26} \text{ erg cm}^{-2} \text{ s}^{-1} \text{ Hz}^{-1} \text{ Mpc}^{-3}$ without applying A_{1600} corrections. This is 1.7 times higher than the value derived by M96, which illus-

¹⁰Infrared Space Observatory

¹¹Space Infrared Telescope Facility

trates the effects of the differing color selections. After correcting for dust absorption we find $\rho_{1600,0} = 1.4 \times 10^{27} \text{ erg cm}^{-2} \text{ s}^{-1} \text{ Mpc}^{-3}$, which is factors of nine and five times higher than the uncorrected values of M96 and M98, respectively. However, this $\rho_{1600,0}$ is still a lower limit because we have not corrected for incompleteness, and we are not sensitive to galaxies having $A_{1600} > 3.6 \text{ mag}$.

This study and other recent observations further demonstrate the close correspondence between local starbursts and high- z Lyman limit systems. Firstly, we find a correlation between β (color) and M_{1600} (UV luminosity) for the U -dropouts, similar to the correlation seen in local starburst galaxies (Heckman et al. 1998). To first order the UV luminosity gives the mass of recently formed stars, while β correlates well with metal content in local galaxies (Heckman et al. 1998). This implies that there is a mass metallicity relationship out to $z \approx 3$. Since the highest luminosity galaxies are clearly reddened they must have produced enough metals to create the dust prior to the epoch of observation. Hence the first epoch of star formation occurred at $z \geq 2.75$ in the most luminous U -dropouts. Secondly, observation of emission lines in the rest frame optical (observed in the near-IR) show that U -dropouts contain ionizing stellar populations to the same degree as local starbursts. This can be seen by comparing the line flux to UV flux density ratios with β for both samples. However, neither the local nor the U -dropout samples show a strong correlations in these diagrams as would be expected from naive application of UV extinction/absorption laws. This suggests that the column density of dust towards HII emission is higher than towards the UV continuum both in local starbursts and out to $z \approx 3$. Consequently, the line flux to UV flux density ratio is not a good indicator of dust ab-

sorption. Thirdly, the marginal detection of two HDF U -dropouts at radio rest $\lambda_0 \approx 1 \text{ cm}$ by Richards et al. (1998) and non-detections of the U -dropouts in the HDF by Hughes et al. (1998) is consistent with estimates of the amount of UV flux reprocessed into the FIR. Deeper observations in both domains (by a factor of $\sim \sqrt{2}$) are required to test the dust reprocessing model proposed here, and to confirm whether the FIR-radio correlation holds at $z \approx 3$.

The methodology presented here is readily adapted to other redshifts. For those sources affected by modest amounts of absorption ($A_{1600} \lesssim 5 \text{ mag}$), the intrinsic UV flux can be recovered from UV quantities alone: flux measurements in two rest frame vacuum-UV bands are sufficient. These observations can also be used to estimate the total UV flux reprocessed into the FIR. Hence, lower limits to the intrinsic $\rho_{UV,0}(z)$ and $\rho_{FIR}(z)$ can be determined. Integration of $\rho_{FIR}(z)$ and comparison to the FIR background spectrum (Fixsen et al. 1998; Hauser et al. 1998) will constrain the amount of star formation totally obscured by dust from the ultraviolet.

We thank two anonymous referees for suggestions that improved this paper. Mark Dickinson, Harry Ferguson, Piero Madau, Chris Martin and Max Pettini stimulated our thinking in numerous discussions. Piero Madau kindly calculated cosmic transmission curves for us. We thank Mark Dickinson for providing the z measurements of the Hawaii and Berkeley groups collated to the HDF V2.0 catalog. This research has made use of the NASA/IPAC Extragalactic Database (NED) which is operated by the Jet Propulsion Laboratory, California Institute of Technology, under contract with the National Aeronautics and Space Administration. This research was supported by NASA grant NAG5-6400.

REFERENCES

- Babu, G.J., & Feigelson, E.D. 1996, "Astrostatistics", Chapman & Hall: London.
- Barger, A.J., Cowie, L.L., Sanders, D.B., Fulton, E., Taniguchi, Y., Sato, Y., Kawara, K., & Okuda, H. 1998, *Nature*, 394, 248
- Baugh, C.M., Cole, S., Frenk, C.S., & Lacey, C.G. 1998, *ApJ*, 498, 504
- Bechtold, J., Yee, H.K.C., Elston, R., & Ellingson, E. 1997, *ApJ*, 477, L29
- Bechtold, J., Elston, R., Yee, H.K.C., Ellingson, E., & Cutri, R.M. 1998, in "The Young Universe: Galaxy Formation and Evolution at Intermediate and High Redshift", Eds. S. D'Odorico, A. Fontana, and E. Giallongo. ASP Conference Series; Vol. 146, p.241 (astro-ph/9802230)
- Bower, R.G., Lucey, J.R., & Ellis, R.S. 1992, *MNRAS*, 254, 601
- Boyle, B.J. & Terlevich, R.J. 1998, *MNRAS*, 293, L49
- Bouchet, P., Lequeux, J., Maurice, E., Prevot, L., & Prevot-Burnichon, M.L. 1985, *ã*, 149, 330
- Brosch, N., Shemi, A., Netzer, H., Blasberger, A., & Topaz, J.M. 1994, in "Advances in multilayer and grazing incidence X-ray/EUV/FUV optics", SPIE, 2279, 469
- Bruzual, A.G., & Charlot, S. 1993, *ApJ*, 405, 538
- Buat, V., & Burgarella, D. 1998, *A&A*, 334, 772
- Burstein, D., & Heiles, C. 1982, *AJ*, 87, 1165
- Burstein, D., & Heiles, C. 1984, *ApJS*, 54, 33
- Calzetti, D. 1997, *AJ*, 113, 162
- Calzetti, D., Kinney, A.L., & Storchi-Bergmann, T. 1994, *ApJ*, 429, 582
- Carlstrom, J.E. & Kronberg, P.P. 1991, *ApJ*, 366, 422
- Connolly, A.J., Szalay, A.S., Dickinson, M., Subbarao, M.U., & Brunner, R.J. 1997, *ApJL*, 486, L11
- Conti, P.S., Leitherer, C., & Vacca, W.D. 1996, *ApJ*, 461, L87
- Dey, A., Spinrad, H., Stern, D. Graham, J.R., & Chaffee, F.H. 1998, *ApJ*, 498, L93
- Désert, F.-X., Boulanger, F., & Puget, J.L. 1990, *A&A*, 237, 215
- Devereaux, N.A., & Eales, S.A. 1989, *ApJ*, 340, 708
- Dickinson, M. 1998, in *The Hubble Deep Field*, eds. M. Livio, S.M. Fall and P. Madau, in press (astro-ph/9802064)
- Eales, S., Lilly, S., Gear, W., Dunne, L., Bond, J.R., Hammer, F., Le Fevre, O., & Crampton, D. 1998, *ApJ*, submitted (astro-ph/9808040).
- Eggen, O.J., Lynden-Bell, D., & Sandage, A.R. 1962, *ApJ*, 136, 748
- Fanelli, M.N., O'Connell, R.W., & Thuan, T.X. 1988, *ApJ*, 334, 665

- Fitzpatrick, E.L. 1986, *AJ*, 92, 1068
- Fixsen, D.J., Dwek, E., Mather, J.C., Bennett, C.L., & Shafer, R.A. 1998, *ApJ*, 508, 123
- Franx, M., Illingworth, G., Kelson, D.D., Van Dokkum, P.G., & Tran, K.-V. 1997, *ApJ*, 486, L75
- Frayser, D.T., Ivison, R.J., Scoville, N.Z., Evans, A.S., Yun, M., Smail, I., Barger, A.J., Blain, A.W., & Kneib, J.-P. 1999, *ApJ*, submitted, (astro-ph/9901311)
- Giavalisco, M., Livio, M., Bohlin, R.C., Macchetto, F.D., & Stecher, T.P. 1996, *AJ*, 112, 369
- Giavalisco, M., Steidel, C.C., & Macchetto, F.D. 1996, *ApJ*, 470, 189
- Gonzalez-Delgado, R., Leitherer, C., Heckman, T.M., Lowenthal, J., Ferguson, H., & Robert, C. 1998, 495, 698
- Guiloteau, S., Omont, A., McMahon, R.G., Cox, P., & Petitjean, P. 1997, *A&A*, 328, L1
- Guiderdoni, B., Bouchet, F.R., Puget, J.L., Lagache, G., & Hivon, H. 1998, *Nature*, 390, 257
- Hauser, M.G. et al., 1998, *ApJ*, 508, 25
- Heckman, T.M., Armus, L., & Miley, G.K. 1990, *ApJS*, 74, 833
- Heckman, T.M., Robert, C., Leitherer, C., Garnett, D.R., & van der Rydt, F., 1998, *ApJ*, 503, 646
- Ivison, R.J., Smail, I., Le Borgne, J.-F., Blain, A.W., Kneib, J.-P., Bézecourt, J., Kerr, T.H., & Davies, J.K. 1998, *MNRAS*, 298, 583
- Helou, G., Khan, I.R., Malek, L., & Boehmer, L. 1988, *ApJS*, 68, 151
- Helou, G. 1991, in *The Interpretation Of Modern Synthesis Observations Of Spiral Galaxies*, edited by N.C. Duric, & P. Crane (ASP, San Francisco), p. 125
- Hibbard, J.E., & Vacca, W.D. 1997, *AJ*, 114, 1741
- Howarth, I.D. 1983, *MNRAS*, 203, 301
- Hughes, D., et al. 1998, *Nature*, 394, 241
- Ivison, R.J. et al. 1998, *ApJ*, 494, 211
- Jarvis, J.F., & Tyson, J.A. 1981, *AJ*, 86, 476
- Kennicutt, R.C., Jr. 1998, *ApJ*, 498, 541
- Kinney, A.L., Bohlin, R.C., Calzetti, D., Panagia, N., & Wyse, R.F.G. 1993, *ApJS*, 86, 5
- Kinney, A.L., Calzetti, D., Bica, E., & Storchi-Bergmann, T. 1994, *ApJ*, 429, 172
- Klaas, U., Haas, M., Heinrichson, I., & Schulz, B. *A&A*, 325, L21
- Kunth, D., Mas-Hesse, J.M., Terlevich, E., Terlevich, R., Lequeux, J., & Fall, S.M. 1998, *A&A*, 334, 11
- Leitherer, C., & Heckman, T.M. 1995, *ApJS*, 96, 9
- Lilly, S.J., Tresse, L., Hammer, F., Crampton, D. & Le Fèvre, O. 1995, *ApJ*, 455, 108
- Lilly, S., Le Fèvre, O., Hammer, F., Crampton, D. 1996, *ApJ*, 460, L1
- Lilly, S., Eales, S., Gear, W. 1998, in "The Next Generation Space Telescope: Science Drivers and Technological Challenges", 34th Liège Astrophysics Colloquium, p. 39
- Lowenthal, J.D., Koo, D.C., Guzman, R., Gallego, J., Phillips, A.C., Faber, S.M., Vogt, N.P., Illingworth, G.D., & Gronwall, C. 1997, *ApJ*, 481, 673
- Madau, P. 1997, in *Star Formation Near and Far*, edited by S.S. Holt & L.G. Mundy, (AIP, Woodbury NY), p. 481
- Madau, P., Ferguson, H.C., Dickinson, M.E., Giavalisco, M., Steidel, C.C., & Fruchter, A. 1996, *MNRAS*, 283, 1388 (M96)
- Madau, P., Pozzetti, L., & Dickinson, M. 1998, *ApJ*, 498, 106 (M98)
- Mas-Hesse, J.M., Arnault, P., & Kunth, D. 1989, *Ap&SS*, 157, 131
- Martin, C., Friedman, P., Shiminovich, D., Madore, B., Bianchi, L., Szalay, A., Heckman, T., Milliard, B., Malina, R., Siegmund, O., Welsh, B., & Rich, M., *BAAS*, 191, 63.04
- McQuade, K., Calzetti, D., & Kinney, A.L. 1995, *ApJS*, 97, 331
- Meurer, G.R., Freeman, K.C., Dopita, M.A., & Cacciari, C. 1992, *AJ*, 103, 60
- Meurer, G.R., Heckman, T.M., Leitherer, C., Kinney, A., Robert, C., & Garnett D.R. 1995, *AJ*, 110, 2665 (Paper I)
- Meurer, G.R., Heckman, T.M., Lehnert, M.D., Leitherer, C., & Lowenthal, J. 1997, *AJ*, 114, 54 (Paper II)
- Mobasher, B., Rowan-Robinson, M., Georgakakis, A., & Eaton, N. 1996, *MNRAS*, 282, L7
- Nota, A., Siriani, M., Leitherer, C., De Marchi, G., & Clampin, M. 1998, *AAS*, 192, 8401.
- Omont, A., Petitjean, P., Guiloteau, S., McMahon, R.G., Solomon, P.M., & Pécontal, E. 1996, *Nature*, 382, 428
- Ortolani, S., Renzini, A., Gilmozzi, R., Marconi, G., Barbu, B., Bica, E., & Rich, M.R. 1995, *Nature*, 377, 701
- Pei, Y.C., & Fall, S.M. 1995, *ApJ*, 454, 69
- Pettini, M., Kellogg, M., Steidel, C.C., Dickinson, M., Adelberger, K.L., & Giavalisco, M. 1998, *ApJ*, submitted
- Rigopoulou, D., Lawrence, A., & Rowan-Robinson, M. 1996, *MNRAS*, 278, 1049
- Richards, E.A., Kellermann, K.I., Fomalont, E.B., Windhorst, R.A., & Partridge, R.B. 1998, *ApJ*, submitted (astro-ph/9803343)
- Sanders, D.B., & Mirabel, I.F. 1985, *ApJ*, 298, L31
- Sawicki, M., & Yee, H.K.C. 1997, 115, 1329
- Searle, L., & Zinn, R. 1978, *ApJ*, 225, 357
- Seaton, M.J. 1979, *MNRAS*, 187, 73p
- Sanders, D.B., Soifer, B.T., Elias, G., Madore, B.F., Matthews, K., Neugebauer, G., & Scoville, N.Z. 1988, *ApJ*, 325, 74.
- Salpeter, E.E. 1955, *ApJ*, 121, 161
- Siriani, M., Nota, A., Leitherer, C., de Marchi, G., & Clampin, M. 1999, *ApJ*, submitted
- Smail, I., Ivison, R.J., & Blain, A.W. 1997, *ApJ*, 490, 5
- Smith, L.F., Biermann, P., & Mezger, P.G. 1978, *A&A*, 66, 65
- Soifer, B.T., Neugebauer, G., Franx, M., Matthews, K., & Illingworth, G.D. 1998, *ApJ*, 501, L171
- Steidel, C.C., & Hamilton, D. 1992, *AJ*, 104, 941
- Steidel, C.C., Pettini, M., & Hamilton, D. 1995, *AJ*, 110, 2519
- Steidel, C.C., Giavalisco, M., Pettini, M., Dickinson, & M., Adelberger, K.L. 1996a, *ApJ*, 462, L17
- Steidel, C.C., Giavalisco, M., Dickinson, M., & Adelberger, K.L. 1996b, *AJ*, 112, 352
- Steidel, C.C., Adelberger, K.L., Giavalisco, M., Dickinson, M., & Kellogg, M. 1998, *Phil.Trans. R.S.*, in press (astro-ph/9805267)
- Storchi-Bergmann, T., Kinney, A.L., & Challis, P. 1995, *ApJS*, 98, 103
- Trentham, N., Sanders, D.B., & Kormendy J. 1999, *AJ*, in press (astro-ph/9901382)
- Williams, R.E., Blacker, B., Dickinson, M., Dixon, W.V.D., Ferguson, H.C., Fruchter, A.S., Giavalisco, M., Gilliland, R.L., Hoyer, I., Katsanis, R., Levay, Z., Lucas, R.A., McElroy, D.B., Petro, L., Postman, M., Adorf, H.-M., & Hook, R.N. 1996, *AJ*, 112, 1335
- Witt, A.N., Thronson, H.A., Capuano J.M. 1992, *ApJ*, 393, 611
- Wright & Pettini, M. 1998, private communication.
- Zepf, S.E., & Ashman, K.M. 1993, *MNRAS*, 264, 611